https://doi.org/10.5194/hess-2021-318
Preprint. Discussion started: 29 June 2021

Hydrology and Earth System Sciences
Discussions

Diagnostic evaluation of river discharge into the Arctic Ocean and its impact on oceanic volume transports

Susanna Winkelbauer[1], Michael Mayer[1,2], Vanessa Seitner[1], Ervin Zsoter[2], Hao Zuo[2], and Leopold Haimberger[1]

[1]Department of Meteorology and Geophysics, University of Vienna, Vienna Austria
[2]European Centre for Medium-Range Weather Forecasts, Reading, United Kingdom

Correspondence: Susanna Winkelbauer (susanna.winkelbauer@univie.ac.at)

Abstract. This study analyses river discharge into the Arctic Ocean using state-of-the-art reanalyses such as the fifth-generation European Reanalysis (ERA5) and the reanalysis component from the Global Flood Awareness System (GloFAS). GloFAS, in it's operational version 2.1, combines the land surface model (Hydrology Tiled ECMWF Scheme for Surface Exchanges over Land, HTESSEL) from ECMWF's ERA5 with a hydrological and channel routing model (LISFLOOD). Further we analyse GloFAS most recent version 3.1, which is not coupled to HTESSEL but uses the full configuration of LISFLOOD.

Seasonal cycles, as well as annual runoff trends are analysed for the major Arctic watersheds - Yenisei, Ob, Lena and Mackenzie - where reanalysis-based runoff can be compared to available observed river discharge records. Further we calculate river discharge over the whole Pan-Arctic region and, by combination with atmospheric inputs, storage changes from the Gravity Recovery and Climate Experiment (GRACE) and oceanic volume transports from ocean reanalyses, try to close the non-steric water volume budget. Finally we provide best estimates for every budget equation term using a variational adjustment scheme.

Seasonal river discharge peaks are underestimated in ERA5 and GloFAS v2.1 by up to 50%, caused by pronounced declining trends due to spurious signals in ERA5s data assimilation system. The new GloFAS v3.1 product exhibits distinct improvements and performs best in terms of seasonality and long term means, however opposing to gauge observations it also features declining trends. Calculating runoff indirectly through the divergence of moisture flux is the only reanalyses based estimate that is able to reproduce the river discharge increases measured by gauge observations (Pan-Arctic increase of 2% per decade). In addition we look into Greenlandic discharge, which makes out about 10% of of the total Pan-Arctic discharge and features strong increases mainly due to glacial melting.

The variational adjustment brought reliable estimates of the volume budget terms on an annual scale, requiring only moderate adjustments of less than 1% for each individual term. Approximately 6584$\pm$84 km^3 freshwater leave the Arctic Ocean per year through it's boundaries. About two thirds of this are recovered through runoff from the surrounding land areas to the Arctic Ocean (4379$\pm$25 km^3 per year) and about one third is supplied by the atmosphere. On a seasonal scale however the variational approach demonstrated that there are systematical errors present in the data-sets, that are not considered in their uncertainty estimation. Hence the budget residuals of some month were too large to be eliminated within the a priori spreads of the individual terms.

https://doi.org/10.5194/hess-2021-318
Preprint. Discussion started: 29 June 2021


Hydrology and Earth System Sciences
Discussions

1 Introduction

Rapid surface warming in the Arctic region has strong impacts on the Arctic water balance and its individual hydrological components, almost certainly leading to an amplification in runoff, evapotranspiration and precipitation (Rawlins et al., 2010; Collins et al., 2014). Increasing river discharge and precipitation trends and intensified sea ice melt coupled with an increase of freshwater inflow through Bering Strait lead to an increase of liquid freshwater stored in the Arctic Ocean (Morison et al., 2012; Haine et al., 2015; Haine, 2020). Ultimately, this could result in enhanced southward exports of low-density waters (Lin et al., 2021) into the Atlantic Ocean, impacting the oceanic circulation also on a global scale. Altogether the hydrological cycle is a complex process with tight coupling between the individual components, having impacts on energy and mass budgets and eventually sea level rise. Therefore the quantification of the individual hydrological components and their changes is of great importance.

With the Arctic Ocean being almost entirely surrounded by landmasses and some of the world's largest rivers draining into it, the link between ocean and surrounding land is remarkably strong. Hence runoff forms one of the key variables in the Arctic freshwater budget. However, direct quantification of river discharge into the Arctic Ocean is aggrevated by the fact that about 30-40% of the Pan-Arctic drainage area is now unmonitored (Shiklomanov et al., 2002). Hydrological monitoring suffered a widespread decline from 74% in 1986 to 67% by 1999 - in Siberia even 73% of river gauges were closed between 1986 and 1999 (Shiklomanov et al., 2002; Shiklomanov and Vuglinsky, 2008). In addition discharge may bypass gauging stations through braided channels or as submarine groundwater and also climatological conditions pose a hindrance to gauge measurements, as they lead to river freeze up in late autumn and flooding in spring due to river-ice break up (Syed et al., 2007).

Atmospheric reanalyses produce gridded estimates of atmospheric and land components, providing spatially continuous estimates of variables such as runoff. They represent a huge advancement in climate monitoring and we want to use this study to evaluate runoff from state-of-the art reanalyses and GloFAS to find a best estimate of Pan-Arctic river discharge and to incorporate it into the Arctics freshwater and volume budget. However data assmilation systems can introduce biases and also inhomogenities due to changes in the observing system are often inevitable (Hersbach et al., 2020). This can lead to spurious jumps in the time series of reanalyzed quantities. This is the case for ERA5s runoff component which features spurious trends in higher latitudes.

The first complete freshwater budget for the Arctic Ocean is proposed by Aagaard and Carmack (1989) and updated by Serreze et al. (2006) and Dickson et al. (2007). Since then, the amount of available data, in particular of atmospheric and oceanic reanalyses, opened new possibilities for evaluation of the coupled oceanic and atmospheric energy and hydrological cycles. For example, Mayer et al. (2019) have presented a greatly improved depiction of the Arctic energy cycle. With regard to freshwater or the water volume budget, the data situation has improved as well. New collections of hydrological data of the far north have been published (Shiklomanov et al., 2021b). Tsubouchi et al. (2012, 2018) presented observation-based estimates of volume fluxes through Arctic gateways. This opens the opportunity to overspecify the Arctic volume budgets and thus also to give residual and bias estimates.

This paper is structured as follows. The next section describes the used data and presents the study domain, followed by the

https://doi.org/10.5194/hess-2021-318
Preprint. Discussion started: 29 June 2021


Hydrology and Earth System Sciences
Discussions

methodology. The results are presented in Sect. 4 and are subdivided into seasonal cycles and trends for the four major Arctic watersheds (Sect. 4.1), Pan-Arctic seasonalities and trends (Sect. 4.2) and an assessment of budget closure by comparison with oceanic fluxes (Sect. 4.3). Section 5 presents conclusions and in the appendix a list of acronyms used throughout the text can be found.

2 Data and study domain

Runoff is taken from the European Centre for Medium-Range Weather Forecast's (ECMWF) 5th generation global climate reanalysis ERA5 (Hersbach et al., 2020), as well as from it's offline simulation ERA5-Land and is downloaded through the Copernicus Climate Change Service (C3S) Climate Data Store (Hersbach et al., 2019; Muñoz Sabater, 2019). Runoff from ERA5 and ERA5-Land are both produced by the land-surface model Hydrology Tiled ECMWF Scheme for Surface Exchanges over Land (HTESSEL, Balsamo et al. (2009)) of the ECMWF Integrated Forecasting System (IFS). However contrary to ERA5, ERA5-Land is not coupled to the atmospheric model of the IFS and no data assimilation is used. An advantage of ERA5-Land is the enhanced global resolution of 9 km (31 km for ERA5) (Muñoz Sabater et al., 2021). Runoff data are converted into river discharge, by integration over the associated domain.

Furthermore we consider the Global Flood Awareness System (GloFAS) river discharge reanalysis. GloFAS is developed by ECMWF and the Joint Research Centre (JRC), as part of the Copernicus Emergency Management Service (CEMS). GloFAS is publically available with data accessible from the Copernicus Climate Change Service Climate Data Store (CDS). Its operational version, GloFAS 2.1 (Harrigan et al. (2019), hereafter denoted GloFAS$_{E5}$), combines a simplified version of the hydrological river routing model LISFLOOD (Knijff et al., 2010), to simulate groundwater processes and river routing, with runoff data from HTESSEL, the land surface model used in ERA5 (Harrigan et al., 2020). In addition we examine an experimental GloFAS version, that also uses LISFLOODs channel routing, but forces it with runoff from ERA5-Land - hereafter denoted GLOFAS$_{E5L}$ - and GloFAS version 3.1 (GLOFAS$_{E5_{new}}$), which uses the full configuration of the LISFLOOD model and is not coupled to HTESSEL but rather produces it's own runoff by using directly precipitation, evaporation and temperature from ERA5. While GLOFAS$_{E5}$ and GLOFAS$_{E5_{new}}$ are available from 1979 to near real time, the experimental version GLOFAS$_{E5L}$ is only available from 1999 to 2018.

Data from ERA5 and GloFAS are compared to available observed river discharge records. Observing records vary among the various countries and rivers, with the longest time series coming from Russia, where discharge monitoring began in the mid 1930s. In contrast discharge measurement in North America did not begin until the 1970s (Holmes et al., 2018). The data used in this study comes from Roshydromet (Ob, Yenisei and Lena) and from the Water Survey of Canada (Mackenzie) and was downloaded through the Arctic Great Rivers Observatory (Shiklomanov et al., 2021b). Table 1 shows coordinates of gauge observations and GloFAS sampling locations for Yenisei, Ob, Lena and Mackenzie. For the Pan-Arctic approach river discharge from additional 20 rivers was taken. Gauging records for Kolyma, Severna Dvina, Pechora and Yukon are available for our period of interest 1981-2019 and are also downloaded through the Arctic Great Rivers Observatory(Shiklomanov et al., 2021b), while records for 16 further rivers are taken from Regional Arctic Hydrographic Network data set (R-ArcticNET, Lammers

https://doi.org/10.5194/hess-2021-318
Preprint. Discussion started: 29 June 2021

Hydrology and Earth System Sciences
Discussions

	Gauges	GloFAS
Yenisei	67.48°N; 86.50°E	67.45°N; 86.45°E
Ob	66.57°N; 66.53°E	66.55°N; 66.45°E
Lena	70.70°N; 127.65°E	72.25°N; 126.75°E
Mackenzie	67.45°N; -133.75°E	67.45°N; -133.75°E

Table 1. Positions of gauge observations and GloFAS locations for Ob, Yenisei, Lena and Mackenzie.

Straits	ORCA
Fram	78.80°-78.80°N,20.60°W-11.50°E
Davis	66.60°-67.30°N, 61.20°-54.00°W
Bering	65.90°-65.70°N, 170.00°-168.30°W
BSO	77.40°-69.70°N, 18.00°-20.40°E
Hecla and Fury	69.85°-70.00°N, 84.50°-84.32°W

Table 2. Start and end points of the sections used for lateral flux calculations on the native ORCA grid.

et al., 2001) for the period 1981-1999.

Atmospheric components like precipitation, evaporation, atmospheric storage change and the divergence of moisture flux (VIWVD) are taken from ERA5 and in Sect. 4.3 we additionally use VIWVD data from the Japanese 55-year Reanalysis JRA55 (Kobayashi et al., 2015) and JRA55 Conventional (Kobayashi et al., 2014). Land storage is derived from snow depth (given as water equivalent) and soil water changes from ERA5.

Oceanic volume fluxes through the main Arctic Gateways are calculated by integrating the cross-sectional velocity component around the Pan-Arctic boundary from the Copernicus Marine Environment Monitoring Service (CMEMS) Global ocean Reanalysis Ensemble Product (GREP, Desportes et al., 2017; Storto et al., 2019), an ensemble of four global ocean reanalyses for the period from 1993 to present. GREP consists of current ocean reanalysis efforts from the Centro Euro-Mediterraneo sui Cambiamenti Climatici (CGLORS, Storto and Masina, 2016), the UK Met Office (FOAM, Blockley et al., 2014), Mercator Ocean (GLORYS, Garric et al., 2017)) and the ECMWF (ORAS5, Zuo et al., 2018, 2019). The four ocean reanalyses are all forced by the ERA-Interim (Dee et al., 2011) reanalysis with different bulk formulas and differences in the data assimilation schemes and observational datasets. For more information see Storto et al. (2019). We also look into the runoff climatology Bt06 (Bourdalle-Badie and Treguier, 2006), that is used in the global ocean-ice model ORCA025. In addition volumetric fluxes are derived from moorings within the so called ARCGATE project (Tsubouchi et al., 2019), covering the period from October 2004 to May 2010. These observation based estimates of volume fluxes come from a mass-consistent framework that views the Arctic Ocean as a closed box surrounded by landmasses and hydrographic observation lines placed in the four major Arctic gateways. The hydrographic lines consist of arrays of moored instruments measuring variables like temperature, salinity and velocity, making it possible to calculate fluxes of volume, heat and freshwater. For more details about the framework see Tsubouchi et al. (2012, 2018).

https://doi.org/10.5194/hess-2021-318
Preprint. Discussion started: 29 June 2021

Hydrology and Earth System Sciences
Discussions
Open Access
EGU

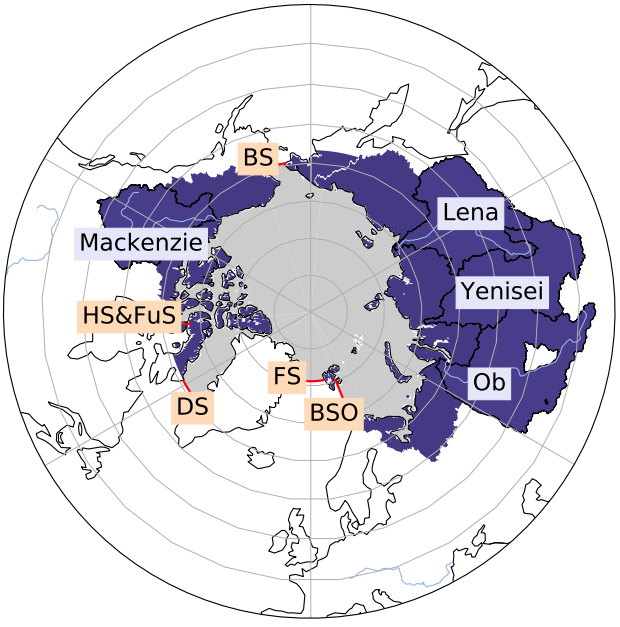

Figure 1. Map of the main study area, consisting of the oceanic area bounded by moorings in Bering Strait (BS), Davis Strait (DS), Fram Strait (FS), the Barents Sea Opening (BSO) as well as Hecla and Fury Strait (HS & FuS) (indicated by grey shading; corresponds to 11.3×10^6 km ^{2}) and the land area draining into it (blue shading; corresponds to 18.2×10^6 km ^{2}). Further the four largest river catchments - Ob, Yenisei, Lena and Mackenzie - are displayed.

Additionally storage terms for land and ocean are calculated using ocean bottom pressure changes and land water storage from GRACE (Gravity Recovery & Climate Experiment) Release 6.0 version 03 from April 2002 to June 2017. Monthly ocean bottom pressure anomalies and land mass anomalies are derived from time-variable gravity observations and are given as equivalent water thickness changes (Landerer, 2020a, b). Satellite observations are processed by three different centers, the Center for Space Research at University of Texas, Austin (CSR), the Jet Propulsion Laboratory (JPL) and the Geoforschungs Zentrum Potsdam (GFZ). We estimate the optimal ocean bottom pressure and land water storage components by taking the mean of those three solutions. Land storage includes the total terrestrial water storage anomalies from soil moisture, snow, surface water, groundwater and aquifers.

Figure 1 presents the study domain. The Arctic Ocean is bounded by moorings in the main gateways. Bering Strait forms the only passage to the Pacific Ocean and delivers low salinity waters into the Arctic, while liquid freshwater and sea ice leave the Arctic Ocean mainly through Fram and Davis Strait. The fourth major strait is the Barents Sea Opening (BSO), where high salinity waters from the Atlantic Ocean are imported into the Arctic. Furthermore there are two small passages, Fury and Hecla Strait, that connect the Arctic Ocean with Hudson Bay.

The terrestrial domain consists of land areas draining into the Arctic Ocean, excluding Greenland but including the Canadian Arctic Archipelago (CAA) as well as islands along the Eurasian coast. At the Pacific passage Yukon and Anadyr rivers are

https://doi.org/10.5194/hess-2021-318
Preprint. Discussion started: 29 June 2021


Hydrology and Earth System Sciences
Discussions

considered, as they build important sources for inflow of low salinity waters into the Arctic Ocean through Bering Strait. The total oceanic and terrestrial areas correspond to 11.3×10^6 km^2 and 18.2×10^6 km^2 respectively. For volume budget analyses we further incorporate Greenlandic discharge and storage change north of Davis and Fram Strait, which adds an additional area of 0.95×10^6 km^2.

3 Methods

3.1 Budget equations

A popular way to calculate the oceanic freshwater budget is through the assumption of a reference salinity. However the outcome is dependent of those reference salinities in a nonlinear way, so that slight differences in the choice of the reference value lead to very different estimates of freshwater transports, both temporally and spatially. Hence Schauer and Losch (2019) declared freshwater fractions not useful for the analysis of oceanic regions and rather recommend the usage of salt budgets for salinity assessments. In this paper we do not calculate salt budgets, but we estimate volume budgets and hence also avoid the usage of a reference salinity. Hereinafter the volumetric budget equations for atmosphere, land and ocean are formulated.

a) Atmosphere

The change of water storage in the atmosphere - here expressed as water vapor integrated from the earths surface to the top of the atmosphere (i.e. total column water vapor; hereafter denoted S_A; atmospheric liquid water and ice are neglected) - denotes the left side of the volumetric budget equation for the atmosphere and is balanced by the surface freshwater fluxes evapotranspiration ET and precipitation P (both in SI units ms^{-1}) and the vertically integrated horizontal moisture flux divergence (last term; hereafter denoted as VIWVD):

$$\frac{\partial}{\partial t}\left(\frac{1}{g\rho_w}\int_0^{p_s} q\,dp\right) = ET - P - \left(\boldsymbol{\nabla}\cdot\left(\frac{1}{g\rho_w}\int_0^{p_s} q\boldsymbol{v}\,dp\right)\right) \tag{1}$$

with the gravitational constant g, surface pressure p_s, specific humidity q, density of freshwater ρ_w and the horizontal wind vector $\boldsymbol{v}$. The equation above is probably more familiar to the reader as a mass budget equation, without ρ_w in the denominator. In order to get volumetric water fluxes, we divided by the density of freshwater ρ_w=1000 kg m^{-3}, which is assumed constant in this paper, neglecting dependence on temperature and soluble substances. Further all terms are integrated over the Arctic area A_{total} to obtain SI units of m^3s^{-1}. For presentation of results, we will often use Sv (=1e6 m$^3s^{-1}$) or km$^3a^{-1}$ as more convenient units.

b) Land

The change in land water storage (S_L) can be expressed as sum of changes of volumetric soil water $SWVL_n$ integrated over the corresponding soil depth l_n and changes in snow depth SD - given as snow water equivalent. Changes in land water storage are balanced through precipitation P$_L$ and evapotranspiration ET$_L$ over land and runoff R (in SI units ms^{-1}). To obtain

https://doi.org/10.5194/hess-2021-318
Preprint. Discussion started: 29 June 2021


Hydrology and Earth System Sciences
Discussions

volumetric fluxes we again perform areal integration over the corresponding area (here the land area A_l).

$$\frac{\partial}{\partial t}\left(SD + \int_{l_n} SWVL_n \, dl_n\right) = P_L - ET_L - R \tag{2}$$

Rearranging Eq. (2) we obtain an estimate of the water discharging into the Arctic Ocean independent of runoff itself. As we prefer analyzed quantities we can further insert Eq. (1) to substitute P and ET, which are derived from short-term forecasts in ERA5, through the analyzed quantities VIWVD and atmospheric storage change:

$$R = -\frac{\partial S_L}{\partial t} + P_L - ET_L = -\frac{\partial S_L}{\partial t} - \frac{\partial S_A}{\partial t} - VIWVD \tag{3}$$

c) Ocean

As per Bacon et al. (2015) the oceanic mass budget equation can be expressed as

$$\iiint_V \frac{\partial \rho}{\partial t} dV = F^{surf} - \iint_{A_{sz}} \rho \boldsymbol{v} \cdot \boldsymbol{n} \, ds \, dz \tag{4}$$

The left side of Eq. (4) denotes the change in mass over a closed volume, F^{surf} describes any surface mass input/output in the form of precipitation, evaporation and runoff. The last term of Eq. (4) expresses ice and ocean side-boundary fluxes from or into the volume (integration is performed along the depth z and the along-boundary coordinate s). Further we apply the Boussinesq approximation and assume ρ as constant. We adopt the reference salinity used in the Nucleus for European Modelling of the Ocean (NEMO) ocean model of ρ_O=1035 kg/m^3 (Madec and Team, 2019) and divide Eq. (4) by ρ_O. This yields an expression where steric effects are ignored and only volume, also considered as Boussinesq mass ($M_O = \rho_O V$), is conserved (Madec and Team, 2019; Bacon et al., 2015):

$$\frac{\partial}{\partial t}\left(\iiint_V dV\right) = P_O - ET_O + R - \iint_{A_{sz}} \boldsymbol{v} \cdot \boldsymbol{n} \, ds \, dz \tag{5}$$

Hence the change of oceanic volume (derived from bottom pressure changes; hereafter denoted S_O) is balanced by precipitation and evapotranspiration over the oceanic domain (P_O and ET_O), runoff from the land domain R and further volume can leave and enter the ocean laterally over it's vertical boundaries, described by the last term of the equation (oceanic lateral transport, denoted F). F is calculated by integrating the cross-sectional velocity component along the side areas of the Arctic boundary. Volume exchange between liquid ocean and sea-ice is conserved in the NEMO model, so we assume sea-ice to be transported by the ocean currents and do not explicitly add ice volume transports to prevent ice transports from being counted twice. Changes in ocean density do not affect the volume as the steric effect is missing due to the Boussinesq approximation.

In this paper we mostly present monthly means, derived by averaging the corresponding fields from reanalyses in their native temporal resolution. Horizontal interpolation and vertical interpolation has been avoided by using all reanalysis products in their native grid representation. Care has been taken also to average over the same area for all products as far as this is possible. The lateral fluxes through the ocean gateways were evaluated along paths on the native ORCA grid that followed the ARCGATE

https://doi.org/10.5194/hess-2021-318
Preprint. Discussion started: 29 June 2021


Hydrology and Earth System Sciences
Discussions
Open Access
EGU

185 mooring arrays as closely as possible - ORCA coordinates are given in table 2. This is essential, since the net lateral volume fluxes in and out of the Arctic are very small (∼0.2 Sv in the annual mean) compared to the fluxes through individual straits (e.g. ∼2.3 Sv for Davis Strait, Curry et al., 2011).

3.2 Variational approach for budget closure

Given all the various, largely independent data sets we use, closure between the budget terms will not be perfect, resulting in a
190 budget residual. In order to get rid of any residual and obtain a closed budget with physical terms only, we follow Mayer et al. (2019), L'Ecuyer et al. (2015) and Rodell et al. (2015) and use a variational Lagrange multiplier approach to enforce budget closure on annual and monthly scales. Therefore the following cost function J is minimized:

$$J = \sum_i \frac{(F_i - F_i')^2}{\sigma_i'^2} + \lambda \sum_i F_i' \tag{6}$$

With the Lagrange multiplier λ, the a priori estimates of the budget terms F_i', the adjusted budget terms F_i, the uncertainty of
195 the respective budget term $\sigma_i'^2$ and the budget residual $\sum_i F_i'$.

a) Annual optimization

Inserting the annual means of the individual budget terms into Eq. (6) and differentiation in respect to λ and the a priori estimates of the budget terms yields eight equations with eight unknowns. Solving the system of equations results in an expression for the adjusted budget terms F_k:

$$F_k = F_k' + \frac{\sigma_k'^2}{\sum_i \sigma_i'^2} \sum_i F_i' \tag{7}$$

Hence the budget residual is distributed across the budget terms according to their relative uncertainty. The a priori uncertainties are derived from the standard deviations of the mean annual budget terms. The a posteriori uncertainties are calculated following Mayer et al. (2018):

$$\sigma_k^2 = \left(\frac{1}{\sigma_k'^2} + \frac{1}{\sum_i \sigma_i'^2 - \sigma_k'^2} \right) \tag{8}$$

205 *b) Monthly optimization*

Monthly optimization is performed in two steps. First adjusted fluxes are calculated for each month separately following Eq. (7), whereat the a priori uncertainty is estimated by taking the maximum of the seasonal standard deviations and is kept fixed throughout all months. However the annual means of the resulting monthly fluxes do not coincide with the annually optimized fluxes. Therefore we follow Rodell et al. (2015) and apply a second Lagrangian optimization, where the adjusted monthly
210 fluxes from the first step (F_k) are adjusted in relation to their uncertainty, so that their annual mean is equal to the annual optimized fluxes F_m:

$$FO_k = F_k + \frac{12\sigma_k'^2}{\sum_i \sigma_i'^2} \left(F_m - \frac{1}{12} \sum_i F_i \right) \tag{9}$$

https://doi.org/10.5194/hess-2021-318
Preprint. Discussion started: 29 June 2021


Hydrology and Earth System Sciences
Discussions

However the second step again generates small monthly residuals. Therefore the whole procedure is performed iteratively a second time, using the a posteriori uncertainties gained through Eq. (8). This results in the desired monthly fluxes, that satisfy both, a closed budget and consistency with the annually optimized fluxes.

3.3 Trend and relative error calculation

We calculate trends following Zsótér et al. (2020) and Stahl et al. (2012) by applying a linear regression to the annual mean time series and calculating trends over a fixed 10 year period:

$$t = \frac{10 * s}{m} \tag{10}$$

With the long term annual means m and the slope s - defined as annual change from the linear regression. Hence t determines the change over a decade relative to the sample mean value. Trends are calculated over the common period of all datasets 1981-2019, except for GloFAS$_{E5L}$ which is calculated over 1999-2018, using annual means and not considering auto-correlation. Significance is determined by using the Wald Test with a t-distribution, where p-values smaller than 0.05 are considered as significant.

To compare river discharge estimates from the various reanalyses to river discharge observations we use the Pearson's correlation coefficient r and a normalised root mean square error (NRMSE), which is calculated by dividing the RMSE through the RMS of the observed values ($NRMSE(x)$=$RMS(x-obs)/RMS(obs)$).

4 Results

We first discuss seasonal cycles and trends for the four major Arctic catchments - Yenisei, Ob, Lena and Mackenzie. Then we extend our assessments to the Pan-Arctic region, where we compare the total terrestrial Arctic runoff with oceanic freshwater fluxes through the main gateways.

4.1 Analysis of major catchments

4.1.1 Seasonal cycles

Figure 2 shows seasonal cycles of various hydrological components for the Yenisei, Ob, Lena and Mackenzie catchments. The top panels compare runoff from ERA5 and ERA5-Land with river discharge from GLOFAS$_{E5}$, GLOFAS$_{E5L}$ and GLOFAS$_{E5_{new}}$ as well as with observed discharge values.

Observations show a distinct runoff peak in June due to snow melt and river ice breakup and weak runoff through winter. The spring flood season of Eurasian rivers depends on the basin size and usually ends by the end of June at small size rivers and by the end of July or beginning of August at large rivers like Ob, Yenisei and Lena (Yang et al., 2007). While smaller rivers usually exhibit a low-flow season in the summer to fall period, discharge from larger rivers mostly shows a slower decrease, also because of summer rainfalls providing additional discharge water. Especially at rivers of Eastern Siberia (e.g. Lena) intense

https://doi.org/10.5194/hess-2021-318
Preprint. Discussion started: 29 June 2021


Hydrology and Earth System Sciences
Discussions

rainfalls in the summer-fall season may occasionally cause rainfall floods (Shiklomanov et al., 2021a). In late winter, with the maximum of river freeze-up, discharge reaches it's minimum.

Runoff data from ERA5 and consequently also from GLOFAS$_{E5}$ clearly underestimate the summer peaks recorded by gauges and reach only about 25 to 50% of the observed peak discharge values. In the low flow season the reanalyses slightly exceed observed discharge, however this does not alter the annual means considerably resulting in a clear underestimation of discharge by ERA5 and GLOFAS$_{E5}$ also in annual terms. The difference between ERA5 runoff and GLOFAS$_{E5}$ discharge is expected to be caused by two sink terms, a groundwater loss component, calibrated in LISFLOOD, that removes water that is lost to deep groundwater systems, and the open water evaporation component, which also removes water through evaporation over water surfaces in LISFLOOD. The negative contribution can reach up to 20-40% of the average flow by any of the two terms in certain regions (described in the LISFLOOD model documentation, Burek et al., 2013). Better accordance in terms of peak height and annual means are achieved by runoff from ERA5-Land - except for the Lena basin - while the sink terms in GloFAS again causes an underestimation by GLOFAS$_{E5L}$. At the Ob basin the runoff peak in ERA5-Land, and also ERA5, occurs in May, thus a month earlier than the observed peak. GloFAS discharge is not in phase with ERA5 runoff, but reaches it's peak in June, presumably due to the delay by the river routing component. In contrast to GLOFAS$_{E5}$ and GLOFAS$_{E5L}$, GLOFAS$_{E5_{new}}$ reaches values similar to observations and agrees best with the observed values in terms of annual means, peak heights and seasonality. Cucchi et al. (2020) run the hydrological model WaterGAP (Müller Schmied et al., 2016) with precipitation, temperature and radiation forcing from ERA5 and from the bias corrected version of ERA5 WFDE5 (Cucchi et al., 2020). Model runs with ERA5 forcing show similar river discharge seasonalities at the Lena catchment as GloFAS$_{ERA5new}$.

The middle panels of Fig. 2 show snowfall and snow melt as well as the atmospheric components net precipitation (P-E) and divergence of moisture flux (VIWVD). Seasonal cycles of P-E and VIWVD minus storage change agree quite well in terms of peak heights and timing, with low moisture inflow and low net precipitation in summer and higher values in autumn and winter. Annual values of P-E and VIWVD-ΔS differ by 2-16% depending on the catchment. Seasonal cycles of ERA5 snow melt show that there is a lag of one month between the peak in snow melt and river discharge. This can partly be explained by the time it takes for the water to reach the river mouth and by water resource management effects, but mostly is caused due to delayed river ice break up in the lower parts of the basins. For example at the upper part of Ob river ice breaks up around April to May, while the lower part breaks up between May and June (Yang et al., 2004b). While human impacts through water withdrawals for agricultural use are rather limited compared to rivers in lower latitudes, water resource management via dams and reservoirs can significantly alter the seasonal discharge cycle of the larger Arctic rivers (Shiklomanov et al., 2021a). Especially the Ob and Yenisei basins, but also Lena and Kolyma, are affected by multiple reservoirs using water for hydroelectric power generation and delaying discharge from high-flow periods to the low-flow season (Lammers et al., 2001; Ye et al., 2003; Yang et al., 2004b, a; Shiklomanov et al., 2021a).

The lower panels of Fig. 2 show land storage change from ERA5 and from GRACE. Additionally ERA5 storage is separated into its components of soil water change ΔS_{SWVL} and snow depth change ΔS_{SD}. In autumn and winter land water is accumulated through a rise in snow depth, in summer storage is lost through snow melt and consequent runoff, and to a smaller part also through evaporation. GRACE shows a significant annual loss of water storage over the past decades, while storage

https://doi.org/10.5194/hess-2021-318
Preprint. Discussion started: 29 June 2021

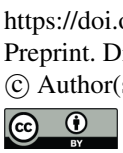

Hydrology and Earth System Sciences
Discussions
Open Access
EGU

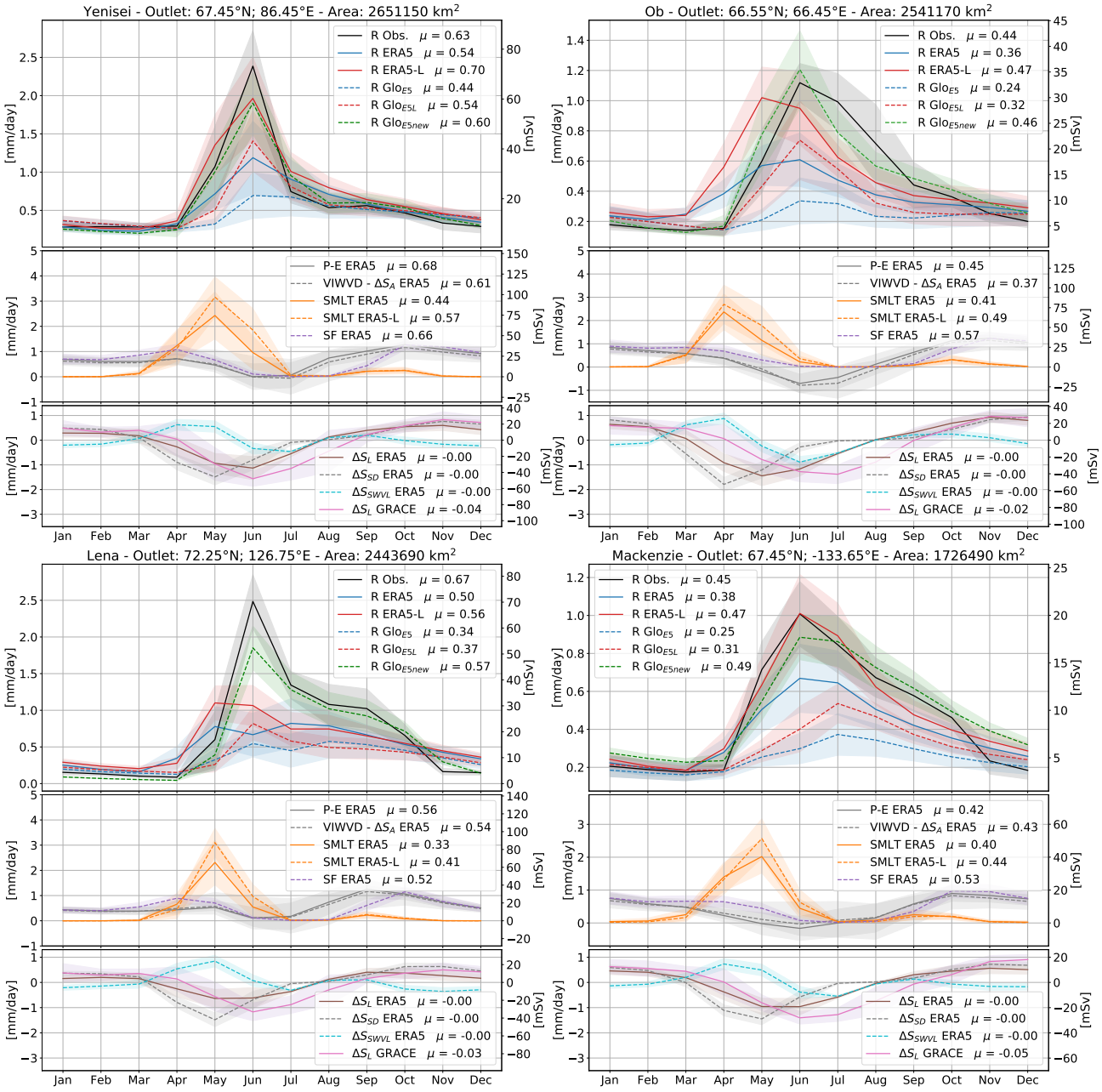

Figure 2. Yenisei, Ob, Lena and Mackenzie seasonal cycles of runoff and river discharge values in the top panel, terrestrial net precipitation (P-E), divergence of moisture flux (VIWVD), snow melt (SMLT) and snowfall (SF) in the middle and land storage change (ΔS_L), snow depth change (ΔS_{SD}) and soil water change (ΔS_{SWVL}) in the bottom panel. Shading denotes variance as the $\pm$ one standard deviation. Furthermore locations of gauge observations and catchment areas are given. Long term annual means in mm/day are given in the legend.

https://doi.org/10.5194/hess-2021-318
Preprint. Discussion started: 29 June 2021


Hydrology and Earth System Sciences
Discussions

change in ERA5 exhibits only a slight annual decline. In terms of seasonality GRACE features the largest storage changes in June and July, while ΔS from ERA5 tends to peak 1-2 month earlier. Again this could be caused by delayed river ice breakup and backwater that is considered in GRACE, but not in ERA5.

4.1.2 Trends

Figure 3 shows annual river discharge values for Yenisei, Ob, Lena and Mackenzie rivers. The corresponding temporal means, standard deviations, decadal trends, normalised RMSEs and correlation coefficients are given in Table 3. Observations indicate a slight increase in river discharge over the past decades. The largest changes occurred at the Ob and Lena basins with a rise of about 4% per decade. Yenisei shows no significant long term trend, as, after a rise until the early 2000s, discharge values seem to have slightly decreased over the past decade. In contrast to observations, runoff from ERA5 and discharge from GLOFAS$_{E5}$ show distinct negative trends of 11 to 16% per decade. These strong decreases are a result of changing biases in the snow assimilation in ERA5 and are discussed further in Sect. 3.3.3. The effect of the sink terms removing water in GLOFAS$_{E5}$, and hence producing a negative shift, results in a strong underestimation towards the end of the time series with values reaching only slightly more than 50 % of the observed values. Runoff from ERA5-Land shows clearly better results, with long term means generally deviating only about 5% from observations (10% for Lena) and quite low normalised RMSE values, however the sink terms in GLOFAS$_{E5L}$ again leads to a clear underestimation of discharge. Calculating runoff indirectly through net precipitation minus land storage change and VIWVD minus atmospheric storage change (Eq. (3)) yield results mostly within 10% of the observed discharge values.

In contrast to GLOFAS$_{E5}$ and GLOFAS$_{E5L}$, river discharge from GLOFAS$_{E5_{new}}$ represents observed discharge from gauges very well and concerning the normalised RMSEs it provides the best results when compared to observations. Both discharge from GLOFAS$_{E5_{new}}$ and estimation through P-E also feature slightly negative trends, only calculation through VIWVD exhibits no, or even slightly positive trends.

4.2 Pan-Arctic approach

To get a complete estimate of the total amount of freshwater entering the Arctic Ocean via land, which is needed for subsequent budget calculation, river discharge is calculated over the whole Pan-Arctic area. First we look into the Pan-Arctic seasonal cycle and afterwards at annual means and long-term trends over the whole Arctic drainage area.

Pan-Arctic freshwater discharge estimates vary significantly between different studies. This comes to a big part from different definitions of the geographic area (Prowse and Flegg, 2000; Shiklomanov and Shiklomanov, 2003) as there is no strict boundary to the south that defines the Arctic and past studies disagree whether to include e.g. Greenland and the Hudson Bay or not. Another reason for discrepancies between different studies comes due to different approaches of discharge evaluation (Shiklomanov et al., 2021a) - some approaches are based on model simulations and others are derived from river discharge measurements. Using only in-situ measurements poses several challenges - especially the handling of the large unmonitored areas, that account for about 30–40% of the total drainage area (Shiklomanov et al., 2002). Most studies adopt the method of hydrological analogy (Shiklomanov and Shiklomanov, 2003) and calculate total discharge by expanding gauged runoff over the

https://doi.org/10.5194/hess-2021-318
Preprint. Discussion started: 29 June 2021

Hydrology and Earth System Sciences
Discussions
Open Access
EGU

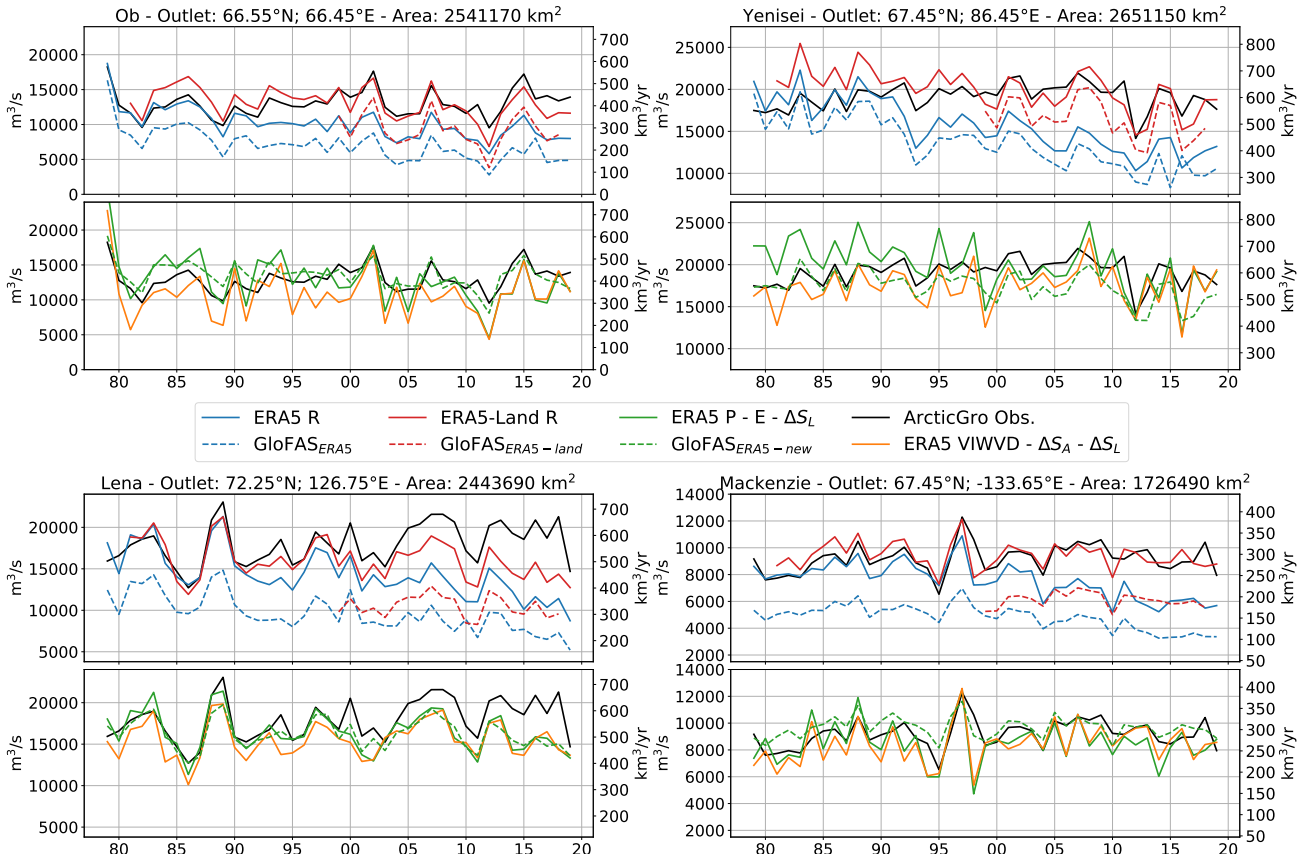

Figure 3. Annual means of observed river discharge, ERA5 runoff, ERA5 net precipitation, ERA5 VIWVD and ERA5-Land runoff as well as GLOFAS$_{E5}$, GLOFAS$_{E5L}$ and GLOFAS$_{E5_{new}}$.

unmonitored area. However hydrological, climatic and land cover conditions between gauged and ungauged areas can differ quite a lot, resulting in inaccurate estimates (Shiklomanov et al., 2021a). Hence we compare two different estimation methods for observed discharge that are displayed in Fig. 4. For that purpose we consider gauging records from the 24 largest Arctic rivers, that amount for roughly 70% of the total drainage area. Pan-Arctic river discharge for the ungauged areas for each month was estimated as follows: Firstly following e.g. Serreze et al. (2006) and applying the method of hydrological analogy for each calendar month by transforming discharge into runoff and, with the assumption that runoff from the ungauged area is the same as runoff from the gauged area, multiplication with the whole drainage area to transform back to river discharge - here denoted as *ae* (area estimate). However taking runoff from reanalysis (e.g. ERA5-Land) for the same 24 drainage areas and expanding it over the whole area yields different results, with smaller summer peaks, than taking runoff directly from the total drainage area. Hence monthly correction factors are calculated from our most reliable products ERA5-Land and GloFAS$_{ERA5new}$ and by multiplication with those, a more accurate estimate of observed Pan-Arctic river discharge should be possible - denoted as

https://doi.org/10.5194/hess-2021-318
Preprint. Discussion started: 29 June 2021

Hydrology and Earth System Sciences
Discussions

		Obs.	E5 R	E5 P-E	E5 VIWVD	E5-L R	Glo_{E5}	Glo_{E5L}	$\text{Glo}_{E5_{new}}$
	μ	19.2	15.5	19.8	17.4	20.0	13.4	16.4*	17.3
	σ	1.5	3.0	2.9	2.4	2.4	2.9	2.3*	1.9
Yenisei	Trend	0.00±0.01^n	-0.14±0.02	-0.06±0.02	0.01±0.02^n	-0.06±0.01	-0.16±0.02	-0.10±0.05*^{n}	-0.05±0.01
	NRMSE		0.25	0.15	0.14	0.11	0.34	0.17*	**0.10**
	r		0.24	0.37	0.49	0.53	0.21	0.81*	**0.64**
	μ	12.9	9.9	12.6	10.6	12.5	6.8	9.3*	13.4
	σ	1.8	1.8	2.9	3.3	2.1	1.7	2.3*	1.7
Ob	Trend	0.04±0.02	-0.11±0.02	-0.08±0.03	0.02±0.04^n	-0.06±0.02	-0.15±0.03	-0.10±0.99*^{n}	-0.03±0.02^n
	NRMSE		0.28	0.21	0.25	0.13	0.45	0.32*	**0.11**
	r		0.39	0.40	0.58	0.66	0.32	0.89*	**0.68**
	μ	18.0	14.2	16.4	15.6	16.1	9.6	10.5*	16.2
	σ	2.5	2.8	2.4	2.2	2.3	2.2	1.3*	1.8
Lena	Trend	0.04±0.02	-0.12±0.02	-0.03±0.02^n	0.00±0.02	-0.05±0.02	-0.15±0.02	-0.03±0.05*^{n}	-0.02±0.02^n
	NRMSE		0.27	0.14	0.17	0.15	0.50	0.45*	**0.14**
	r		0.33	0.65	0.74	0.66	0.27	0.73*	**0.76**
	μ	9.2	7.5	8.6	8.5	9.4	4.8	6.1*	9.7
	σ	1.0	1.3	1.5	1.5	1.0	0.9	0.5*	0.7
Mackenzie	Trend	0.02±0.02	-0.11±0.02	-0.01±0.03^n	0.03±0.02	-0.02±0.01^n	-0.13±0.02	-0.00±0.04*^{n}	-0.01±0.01^n
	NRMSE		0.24	0.17	0.16	0.09	0.49	0.36*	**0.09**
	r		0.29	0.49	0.55	0.65	0.35	0.65*	**0.73**

Table 3. Mean values and standard deviations of river discharge in units $10^3 \text{m}^3\text{s}^{-1}$ as well as relative decadal trends and their standard errors (see Eq. (10)), calculated over the period 1981-2019 (1999-2018 for GLO_{E5L}, indicated by the superscript *). Trends that are not significant are marked with an superscript ^{n}. Additionally normalised RMSE values and correlation coefficients for annual means are given. Bold values identify the best correlation coefficients and NRMSE values.

Ee (ERA estimate) and *Ge* (GloFAS estimate), leading to more plausible high flow peaks. Following the results of the previous sections we trust most in $\text{GloFAS}_{ERA5new}$ as it featured the smallest NRMSEs and highest correlation coefficients and hence use the GloFAS estimate *Ge* for the following Pan-Arctic analysis.

4.2.1 Seasonal Cycle

Figure 5 shows the mean seasonal cycles of the various Pan-Arctic river discharge estimates for the period 1981 to 2019 (1999 to 2018 for $GLOFAS_{E5L}$).

Results are similar as for the individual catchments, with large amounts of water entering the Arctic Ocean in June. Observations (*Ge*) show summer peaks of about $4.8 * 10^5$ m^3s^{-1} and annual means of 4031 $\text{km}^3\text{yr}^{-1}$. ERA5 runoff and discharge from $GLOFAS_{E5}$ and $GLOFAS_{E5L}$ clearly underestimate the summer peaks and annual means, however they slightly overestimate runoff in the low flow winter months. ERA5-Land runoff performs quite well in terms of annual means, but the June

https://doi.org/10.5194/hess-2021-318
Preprint. Discussion started: 29 June 2021

Hydrology and Earth System Sciences
Discussions

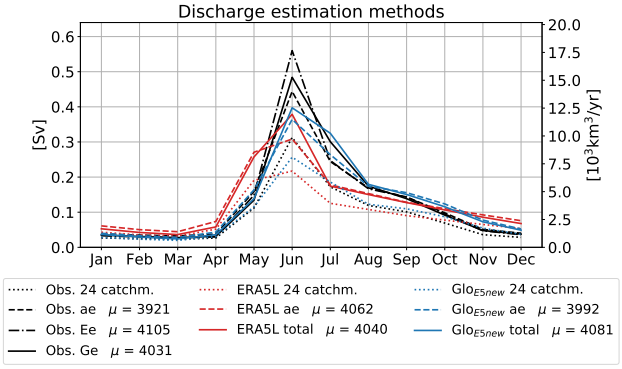

Figure 4. Pan-Arctic discharge estimates using hydrological analogy (ae) and monthly correction factors from ERA5-Land (Ee) and GloFAS$_{ERA5new}$ (Ge). Long term annual means in km^{3}yr^{-1} are given in the legend.

maximum is still about 25-35% too low. $GLOFAS_{E5_{new}}$ performs best in terms of seasonality, but still slightly underestimates the summer peak. Indirectly calculated discharge through Eq. (3) does not reach those distinct high June peaks. Annual values from calculation of P-E reach values similar to ERA5-Land runoff, while the VIWVD estimate is about 5% too low. The runoff climatology Bt06 exhibits a similar seasonal cycle as our observation based estimate, however it is roughly 9% lower than our estimate.

The bottom panel of Fig. 5 shows land storage change components. The time lag between the observed storage change through GRACE and ERA5 is clearly evident again. And just as for the four major basins, also the Pan-Arctic area shows a major decline of land water storage over the past decades, reaching -132 km^3 per year for our area of interest, while land storage from ERA5 shows considerably smaller declines of -34 km^3 per year. The largest changes for GRACE water storage occur over the Canadian Arctic Archipelago and the mountainous areas of Mackenzie and Yukon basin, suggesting a tight linkage to glacial melting. Additionally Greenland features a storage decline of -134 km^3 per year, accounting for roughly 50% of the total storage change. Wouters et al. (2019) use monthly GRACE Stokes coefficients to examine global glacier mass losses for regions defined in the Randolph Glacier Inventory (RGI), excluding Greenland. Building the sum over all regions that roughly resemble our area of interest, yields a glacial mass change of about -100 Gt (gigatons), or roughly -109 km^3 per year. Hence the sum of glacial mass change and storage change from ERA5 resembles the land storage change from GRACE within 10%.

4.2.2 Trends

Long term means of annual discharge over the coinciding period of all datasets 1999-2018 (1981-2018 in brackets) and the distribution to Eurasia, North America and the CAA can be seen on the left panel of Fig. 6 and long term annual means, relative trends, correlation coefficients and NRMSE values are provided in Table 4. About 75 % of Pan-Arctic runoff come from the Eurasian watersheds, followed by North America with about 17 % and the smallest contribution coming from the CAA. Total Pan-Arctic runoff values, calculated over 1999-2018, range between 2625 km^{3}yr^{-1} for $GLOFAS_{E5}$ and 3952 km^{3}yr^{-1} for

https://doi.org/10.5194/hess-2021-318
Preprint. Discussion started: 29 June 2021

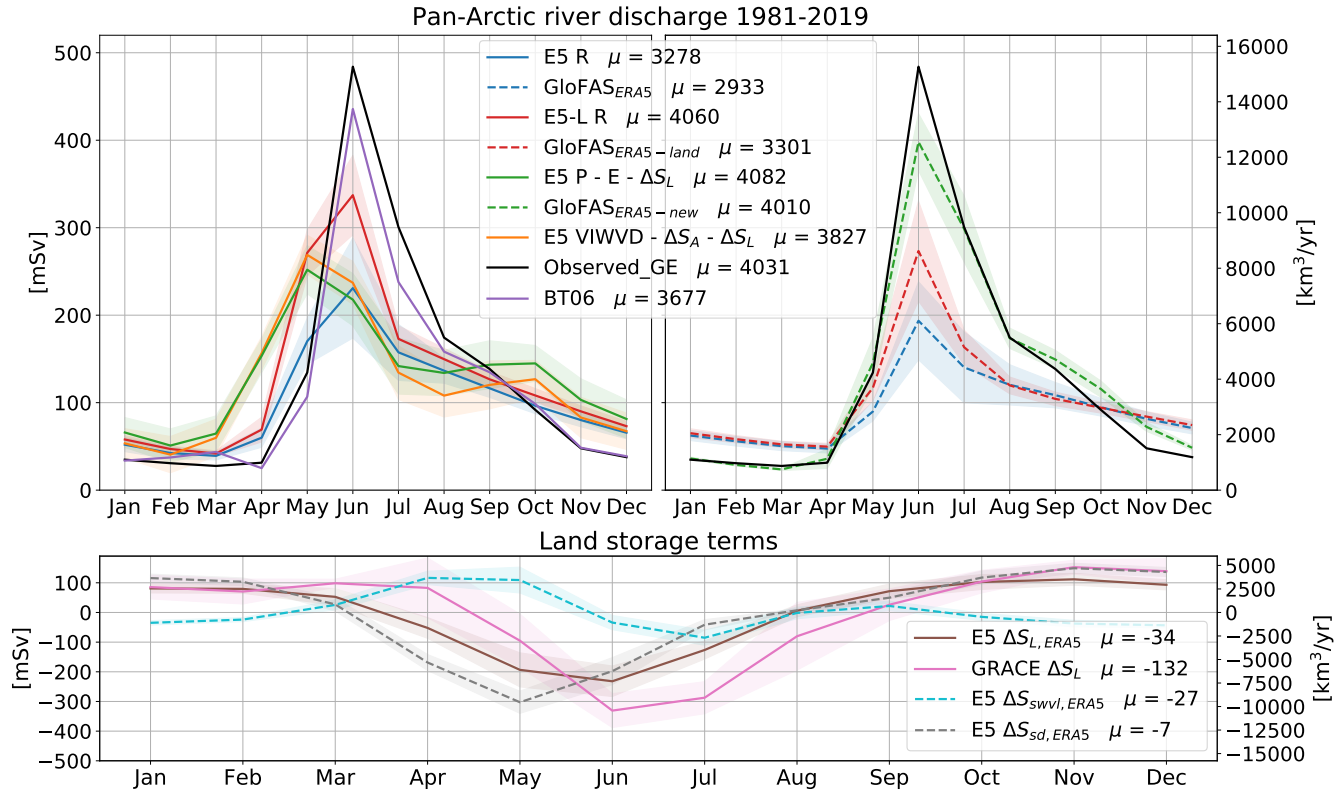

Figure 5. Top panel: Seasonal Cycles of Pan-Arctic runoff for ERA5, ERA5-Land and various GloFAS versions, as well as indirectly calculated runoff through P-E and VIWVD. Additionally an estimate of observed river discharge is given. Seasonal Cycles are calculated over the period 1981-2018 (1999-2018 for $GLOFAS_{E5L}$). Bottom panel: storage change components from GRACE and ERA5. Shading denotes variance as the ± one standard deviation. Additionally long term annual means in km^{3}yr^{-1} are given and appropriately the right axis is scaled in km^{3}yr^{-1}.

indirectly calculated runoff through P-E-ΔS_L from ERA5. Our observation based estimates are considerably higher, reaching 4117 km^{3}yr^{-1}. Using observations of river discharge only and omitting the CAA, Serreze et al. (2006) obtain values of 3200 km^{3}yr^{-1}. Including the CAA, but excluding Yukon river, Haine et al. (2015) combine runoff from ERA-Interim with river discharge observations and report annual values of 3900 ± 390 km^{3}yr^{-1} for the period 1980-2000 and 4200 ± 420 km^{3}yr^{-1} for the period of 2000-2010. Our observation based estimates, including Yukon river, reach values of 3971 ± 31 km^{3}yr^{-1} for 1980-2000 and 4155 ± 42 km^{3}yr^{-1} for 2000-2010. Subtracting the contribution of Yukon River (about 200 km^{3}yr^{-1}), our estimates are about 5% lower than those from Haine et al. (2015). Excluding Yukon river for ERA5-Land runoff and indirectly calculated runoff through ERA5 P-E, both estimates are quite close to the estimates made by Haine et al. (2015) for the period of 1981-2000, however they are substantially too low in the 2000-2010 period. ERA5 and $GLOFAS_{ERA5}$ feature far too low values for both periods.

https://doi.org/10.5194/hess-2021-318
Preprint. Discussion started: 29 June 2021

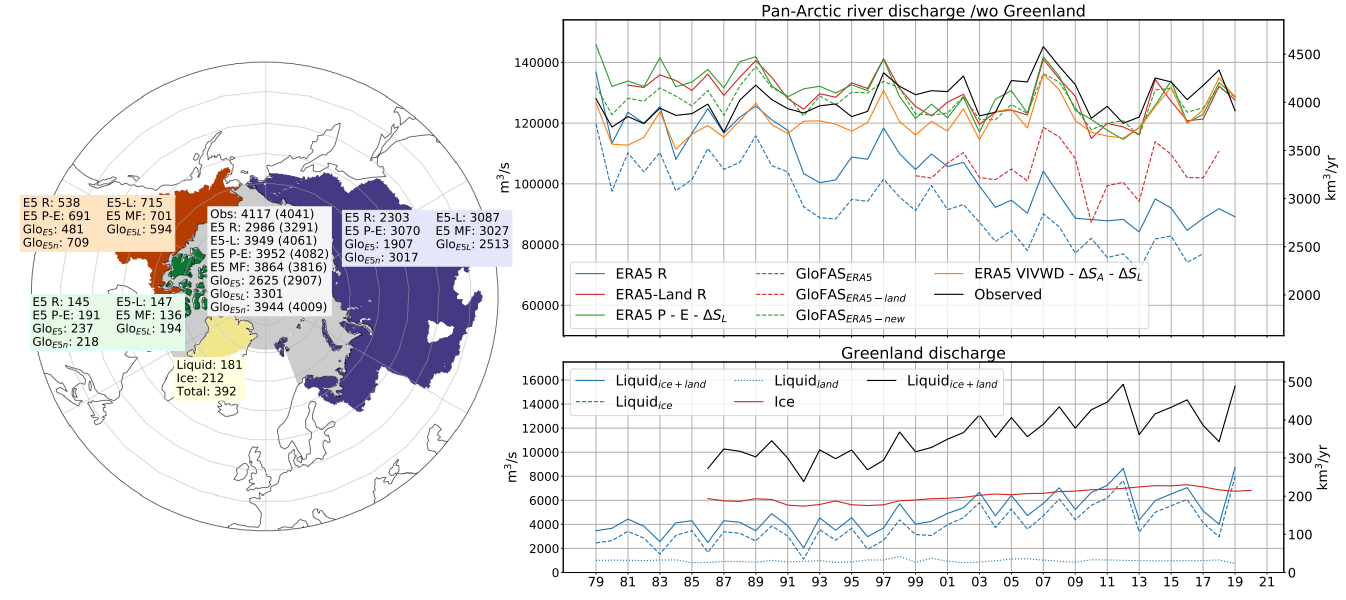

Figure 6. The left panel shows the drainage area and mean annual discharge values in km^{3}yr^{-1} for the whole area, as well as for Eurasia, North America and the CAA individually. Values are calculated over the coinciding period of all datasets 1999-2018 (values in brackets are calculated over the period 1981-2018). On the right hand side annual means of our observation based estimate, ERA5, ERA5-Land, $GLOFAS_{E5}$, $GLOFAS_{E5L}$ and $GLOFAS_{E5_{new}}$ runoff, as well as indirectly calculated runoff through P-E and VIWVD are shown. Additionally Greenlandic liquid (from land and ice) and solid discharges are displayed in the bottom right panel.

For the whole Pan-Arctic region, both ERA5 and $GLOFAS_{ERA5}$ feature runoff decreases of 10-11 % per decade, while ERA5-Land and indirectly calculated runoff through ERA5 P-E exhibit negative trends of about 2-3 % per decade. In contrast the runoff estimate through ERA5's VIWVD features a slight increase of 2%, identically to the trend present in our observation based estimate. GloFAS$_{ERA5new}$ comes closest to gauge observations concerning annual means and NRMSE values, while indirectly calculated runoff through VIWVD features the same trend as observations and also the highest correlation concerning annual means. However the VIWVD estimate generally yields a roughly 5% lower discharge.

The strong decreases in ERA5 runoff are reinforced through two discontinuities in the dataset, one around 1992 and the second one around 2004, that lead to a significant drop and hence a clear underestimation of runoff over the past decades. As $GLOFAS_{E5}$ takes ERA5 as input, it also adopts those discontinuities. In contrast ERA5-Land does not exhibit such breaks, suggesting that the error may come from the data assimilation system in ERA5. While the discontinuity around 2004 was traced back to the introduction of the IMS (Interactive Multisensor Snow and Ice Mapping System) snow product into the assimilation system (Zsótér et al., 2020), the reason for the break around 1992 could not be identified yet and is discussed further in the following section.

Contrary to discharge estimates from reanalyses, observations show opposing trends and a rise in river discharge over the past decades. In NOAAs Arctic Report Card 2018 Holmes et al. (2018) stated that river discharge from Eurasians largest rivers (Ob,

https://doi.org/10.5194/hess-2021-318
Preprint. Discussion started: 29 June 2021

Hydrology and Earth System Sciences
Discussions

		Observed Ge	E5 R	E5 (P-E)	E5 VIWVD	E5-L R	Glo_{E5}	Glo_{E5L}	$Glo_{E5_{new}}$
	μ	127.8	104.4	129.4	121.0	128.8	92.2	104.7*	**127.1**
	σ	6.1	13.0	7.1	5.9	6.6	11.3	7.0*	5.1
Pan-Arc.	Trend	0.02±0.01	-0.10±0.01	-0.03±0.01	**0.02±0.01**	-0.02±0.01	-0.11±0.01	$0.00\pm0.03^{*n}$	-0.01±0.01
	NRMSE	-	0.22	0.06	0.06	0.06	0.30	0.20*	**0.04**
	r	-	-0.14	0.29	**0.78**	0.38	-0.15	0.85*	0.53

Table 4. Mean values and standard deviations of Pan-Arctic river discharge in $m^3 s^{-1} * 10^{-3}$ as well as decadal relative trends, calculated over the period 1981-2019 (1999-2018 for $GLOFAS_{E5L}$, indicated by *). Trends that are not significant are indicated by the superscript ^{n}. Bold values identify the best estimates in respect of long term means, trends, correlation coefficients, NRMSE values

Yenisei, Lena, Kolyma, Pechora, Severnaya Dvina) has increased by 3.3 ± 1.6 % per decade since 1976 and by 2.0 ± 1.8 % per decade for the largest North American rivers (Mackenzie and Yukon). Our observation based estimates show an increase of 2 ± 1% for the whole Pan-Arctic region.

While runoff from Greenland was left out so far, contributions of land and ice discharge are not negligible. Additionally to Eurasian and North American discharge, Fig. 6 shows discharge from the Greenlandic ice and land areas north of our boundaries in Davis and Fram Strait. Greenlandic liquid discharge from land and ice is taken from Mankoff et al. (2020a), who calculate discharge from daily runoff estimates of the Modèle Atmosphérique Régional (MAR) and the Regional Atmospheric Climate Model (RACMO). We estimate the optimal discharge by taking the mean of MAR and RACMO discharge. Solid ice discharge through calving of marine-terminating glaciers and melt-water from ice–ocean boundary melting at submarine glaciers is taken from Mankoff et al. (2020b) over the regions central west (CW), north west (NW) and north (NO) (see Mankoff et al. (2020b), their Fig. 1) to roughly account for our region of interest. With a total contribution of 392 $km^3 yr^{-1}$ over the period 1999-2018, discharge from Greenland accounts for roughly 10% of total Pan-Arctic discharge. Most of the freshwater supplied to the Arctic Ocean comes from solid ice discharge, followed by liquid discharge from glaciers and only a small contribution from land runoff. Liquid discharge from land and ice show pronounced seasonalities with peaks in June and July, while solid ice discharge stays continuous throughout the year. The bottom figure of the right panel of Fig. 6 shows annual means for the individual Greenlandic discharge components and Table 5 displays mean values and trends. Liquid ice discharge exhibits a vast positive trend of 26% per decade and also solid ice discharge shows a clear rise of about 8% per decade. It can be expected that Greenland discharge will further increase in the future (Muntjewerf et al., 2020; Church et al., 2013; Vaughan et al., 2013, e.g.)

Adding Greenlandic discharge to our *Ge* observation estimate, yields a total discharge of 4423 $km^3 yr^{-1}$. A recent assessment (Shiklomanov and Lammers, 2013; Shiklomanov et al., 2021a) estimates the total discharge to the Arctic Ocean at approximately 4300 $km^3 yr^{-1}$ for the period 1936-2006. Differences may stem from slight variations in discharge area - Shiklomanov and Lammers (2013) use an area of approximately 19×10^6 km^2, while our area together with the considered Greenlandic area (0.95×10^6 km^2) sums up to 19.15×10^6 km^2 - and from different calculation periods. Discharge was very likely smaller in the mid-20th century.

https://doi.org/10.5194/hess-2021-318
Preprint. Discussion started: 29 June 2021

Hydrology and Earth System Sciences
Discussions

		Liquid_{Ice}	Liquid_{Land}	Liquid_{total}	Ice	Total
Greenland	μ	4.2	1.0	5.2	6.7	11.9
	σ	1.5	0.1	1.5	0.5	2.0
	Trend	0.25±0.05	0.01 ± 0.02^n	0.20±0.04	0.08±0.01	0.13±0.02

Table 5. Mean values, standard deviations and trends for liquid discharge from ice and land as well as solid ice discharge for Greenland north of Davis and Fram Strait over the period 1987-2019. Trends that are not significant are indicated by the superscript ^{n}.

4.2.3 ERA5 Runoff discontinuities

As mentioned above, a possible reason for the negative shifts in ERA5 runoff lies in the data assimilation system and its removal of soil moisture. Zsótér et al. (2020) assess the $GLOFAS_{E5}$ river discharge reanalysis as well as ERA5 and ERA5-Land runoff and compare them with available river discharge observations. Similarly to our diagnostics for Arctic rivers, Zsótér et al. (2020) find river discharge decreases in GloFAS-ERA5 for several rivers of the world, that are not supported by observations. They find trends in tropical and subtropical areas being driven by changes in precipitation, while changes in snow melt have a very strong influence on river discharge trends in the northern latitudes. Thus the runoff decreases in the northern latitudes are likely linked to snow assimilation and other processes related to snow melt. Figure 7 shows ERA5 snowfall, snow melt and the sum of snow melt and snow evaporation as well as the corresponding parameters from ERA5-Land for the whole Pan-Arctic region, Eurasia, North America and the CAA. ERA5 shows great differences between snow gain and snow loss and Pan-Arctic snow melt exhibits the same discontinuities around 1992 and 2004 as runoff from ERA5. In contrast snow gain and snow loss are in balance for ERA5-Land. Zsótér et al. (2020) find similar results and attribute the differences to the land data assimilation, that has impacts on snow and soil moisture. The discontinuity in 2004 was traced back to a change in operational snow analysis, through the introduction of the 24-km Interactive Multi-Sensor Snow and Ice Mapping System (IMS) snow cover information to the snow assimilation system in 2004 (Zsótér et al., 2020). While the discontinuity around 2004 is present in the Eurasian watershed as well as in North America, the discontinuity around 1992 is only present in Eurasia. Figure 8 shows the spatial distribution of the snow melt discontinuities, calculated as differences between snow melt climatologies from 1979-1991 and 1992-2003, as well as 1992-2003 and 2004-2019. The latter difference exhibits spurious signals at the coastal mountain range of Alaska, the Rocky Mountains and at mountainous regions in Siberia, the prior discontinuity spots rather random signals only over Eurasia.

4.3 Comparison with oceanic fluxes

In this section we look at the oceanic volume budget as described in Eq. (5). For this purpose we calculate volumetric fluxes through the oceanic gateways - BSO, Fram, Davis, Bering, Hecla and Fury Strait - using ocean reanalyses and compare them to our various freshwater input estimates. Oceanic storage change is derived from ocean reanalyses and from GRACE. To close the budget and get rid of any residuals we use a variational approach (see Sect. 2.1.2).

Figure 9 shows seasonal cycles of lateral net volume fluxes from ORAS5 and from the GREP ensemble for 1993-2018

https://doi.org/10.5194/hess-2021-318
Preprint. Discussion started: 29 June 2021

Hydrology and Earth System Sciences
Discussions
Open Access
EGU

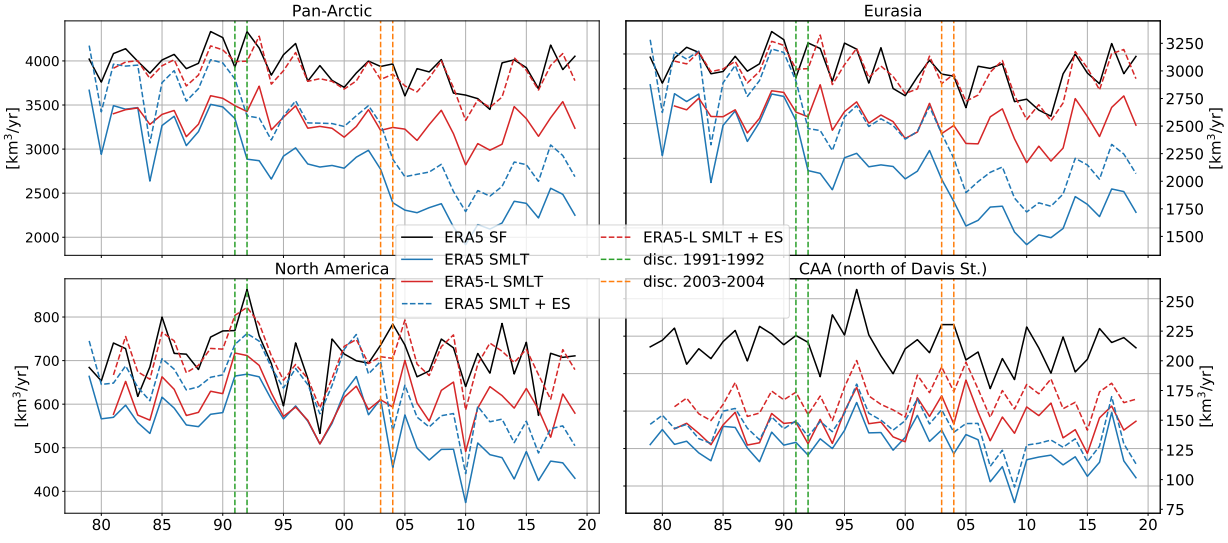

Figure 7. Annual means of ERA5 snowfall (SF, black), ERA5 snow melt (SMLT, blue) and the sum of ERA5 snow melt and snow evaporation (SMLT+ES, blue dashed) as well as ERA5-Land snow melt (red) and ERA5-Land SMLT+ES (red, dashed) for the whole Pan-Arctic region (top left), Eurasia (top right), North America (bottom left) and the CAA (bottom right).

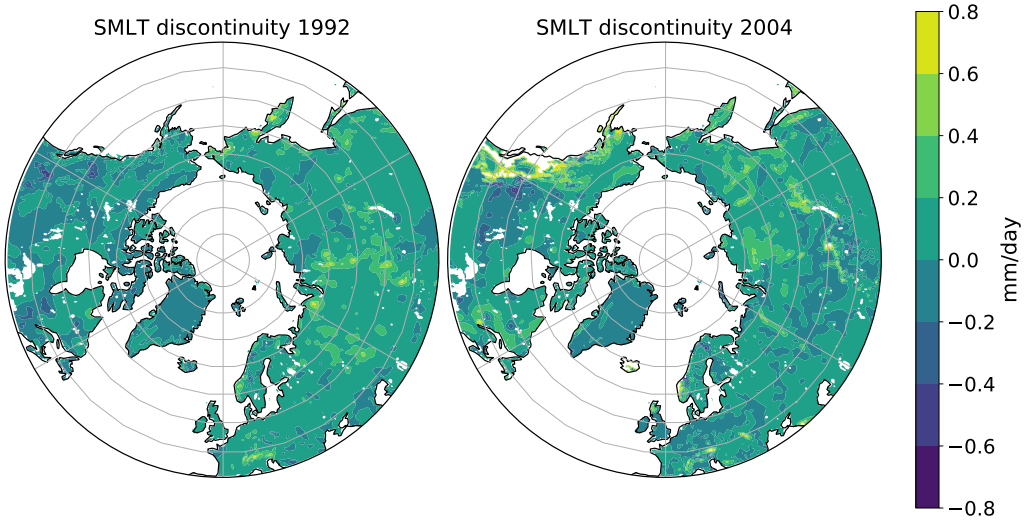

Figure 8. ERA5 snow melt discontinuities, calculated by subtracting the long term SMLT means from 1979-1991 and 1992-2003 and respectively 1992-2003 and 2004-2019.

https://doi.org/10.5194/hess-2021-318
Preprint. Discussion started: 29 June 2021


Hydrology and Earth System Sciences
Discussions

The GREP ensemble shows an annual mean lateral transport out of the Arctic region of $0.207 \pm 0.048 Sv$, with ORAS5 being on the higher end of the ensemble with an annual outflow of $0.238 Sv$ and a summer peak of $0.578 Sv$. The seasonal cycles of the oceanic volume transports resemble the seasonal cycles of the freshwater input and peak in June, as the ocean reacts almost instantly to surface freshwater input and generates barotropic waves that lead to mass-adjustment in about a week (Bacon et al., 2015).

In addition to the oceanic transports the left panel of Fig. 9 shows the forcing terms involved in the generation of the ORAS5 fluxes:

$$F_{ORAS5} = (P_O - ET_O)_{ERAInterim} + R_{BT06} - \frac{\partial S_{ORAS5}}{\partial t} + damp_{ORAS5} + FW_{adj} \tag{11}$$

Next to net precipitation from ERA-Interim and river discharge from the BT06 climatology, we need to add a surface salinity damping term ($damp_{ORAS5}$), which represents an additional non-physical surface freshwater forcing in the ocean reanalyses (last term of Eq. 6.1 in Madec and Team, 2019). Additionally a freshwater adjustment term (FW_{adj}) should be added due to the assimilation of global mean-sea-level changes. This term is not separately saved as model output in ORAS5 and hence is not considered in our analysis (therefore it is marked grey in Eq. (11)). However we deem the freshwater adjustment term as a rather small source of error and nevertheless would expect good closure concerning Eq. (11). With an annual deviation of $0.005 Sv$ and an NRMSE value of 0.19 the accordance between ORAS5 and it's freshwater input estimate is fairly reasonable. Next to the FW adjustment term, another cause for the discrepancies between forcing and computed volume fluxes is that the ocean reanalyses compute their own turbulent air-sea fluxes (REF) and do not use that from ERA-Interim. However, given the generally low values of sensible and latent heat fluxes in the Arctic we consider this a moderate source of error.

The right panel of Fig. 9 shows various estimates of freshwater input minus oceanic storage change. To estimate the atmospheric freshwater input over the ocean we take net precipitation from ERA5 as well as VIWVD from ERA5, ERA-Interim, the Japanese 55-year Reanalysis JRA55 and JRA55 Conventional. For the reanalysis-based estimates we use the river discharge reanalyses we have most confidence in, namely $GloFAS_{ERA5new}$, ERA5-Land runoff and the indirect estimates through P-ET and VIWVD minus storage change. Land storage is only derived from GRACE, while oceanic storage is taken from GRACE and from ORAS5. GRACE and ORAS5 show quite similar seasonal cycles, with mass being accumulated by the ocean in summer and released in winter, most likely caused by the seasonal variation of wind stress curl and seasonal changes in Ekman pumping (Bacon et al., 2015), however they disagree in terms of annual trends, as ORAS5 indicates a slight increase of mass over the past decades, while GRACE points to a decrease. The observation based estimates are calculated using river discharge from our observation estimates (*ae, Ee, Ge*) and oceanic storage change from GRACE. The atmospheric components VIWVD and atmospheric storage change over the ocean are still taken from reanalyses (ERA5, ERA-Interim, JRA55, JRA55c), as we lack the corresponding observations. Greenlandic discharge is taken from Mankoff et al. (2020a, b). Calculating the mean over our reanalyses and observation based estimates we obtain annual values of $0.208 \pm 0.004 Sv$ and $0.210 \pm 0.003 Sv$, respectively. Thus, compared to the GREP volume flux we get an imbalance of $0.001 - 0.003 Sv$, accounting for roughly 1% of the fluxes.

Figure 10 shows the budget residuals, calculated as GREP ensemble average volume transport minus the various freshwater estimates. From January to April residuals are generally positive, as the freshwater input from atmosphere and land is low due

https://doi.org/10.5194/hess-2021-318
Preprint. Discussion started: 29 June 2021

Hydrology and Earth System Sciences
Discussions
Open Access
EGU

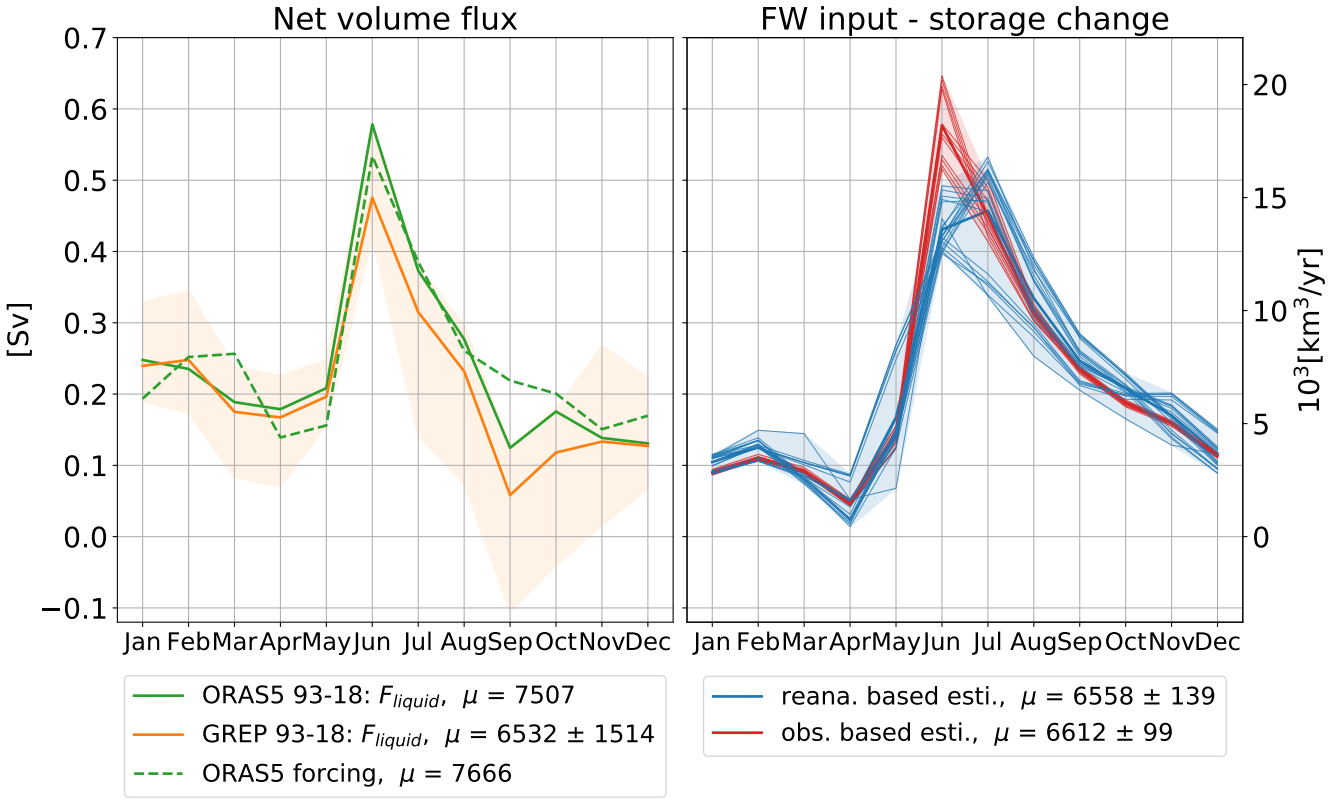

Figure 9. Left panel: Mean seasonal cycles of lateral net volume fluxes (defined positive out of the Arctic) from ORAS5 (1993-2018) and GREP (1993-2018), as well as the sum of forcing terms generating ORAS5. Right panel: Observation and reanalyses based estimates of freshwater input minus oceanic storage.

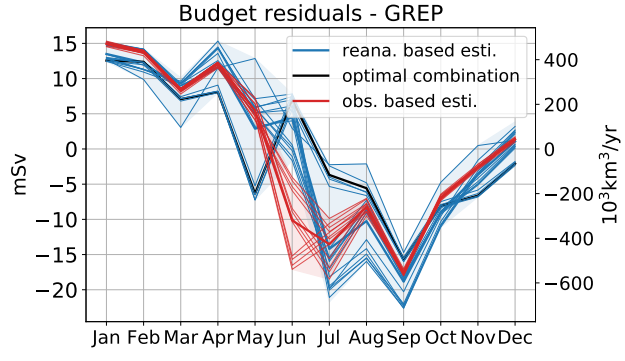

Figure 10. Mean annual cycles of different realisations of the budget residuals (reanalyses based: blue lines, observation based: red lines) and the optimal combination yielding the smallest NRMSE value (black line).

https://doi.org/10.5194/hess-2021-318
Preprint. Discussion started: 29 June 2021

Hydrology and Earth System Sciences
Discussions

	GREP	ORAS5	ORAS5 forcing	ARCGATE	reana. based estimate	obs. based estimate
μ	0.207/0.203*	0.238/0.227*	0.243	0.151*	0.208	0.210
NRMSE	-	0.218^{1}	$0.327^{1}/0.195^{2}$	$0.813^{1*}/0.857^{2*}$	$0.457^{1}/0.376^{2}$	$0.491^{1}/0.347^{2}$
r	-	0.971^{1}	$0.856^{1}/0.928^{2}$	$-0.313^{1*}/-0.522^{2*}$	$0.605^{1}/0.739^{2}$	$0.732^{1}/0.855^{2}$

Table 6. 1993-2018 (*2004-2010) long term means, NRMSEs and correlation coefficients of oceanic volume transports from GREP, ORAS5 and ARCGATE, as well as estimates derived from the forcing terms used in ORAS5 (as described in Eq. (11)). Additionally our reanalyses and observation based estimates are given. NRMSE values and correlation coefficients are calculated using monthly means and in respect to GREP(^{1}) and ORAS5(^{2}). Units are Sverdrup (Sv).

to river icing and low precipitation values, however freshwater that entered the Arctic in the past season and moves slowly with the ocean currents still find it's way through the Arctic gateways. In June, the large freshwater peak generates barotropic waves that are also seen in the reanalysis volume transports, residuals arise from different river discharge estimates and are generally positive for reanalyses and negative for observation based estimates. In late summer river discharge tends to decline and precipitation adopts the main role of delivering freshwater to the ocean. Oceanic reanlyses show a fast decline after the June peak and exhibit a volume transport minimum in September leading to a negative residual peak in all estimates. We assume that volume that enters the Arctic as freshwater through precipitation is slowly transported with the ocean currents and modified by wind stress, partly freezes on the way and takes weeks up to month to leave the Arctic area, explaining the elevated winter and spring transports.

Table 6 shows annual means of the various transport estimates, standard deviations and NRMSEs. The normalised RMSE values are calculated with respect to GREP (^{1}) and ORAS5 (^{2}), indicated by the superscripts. In addition to the estimates from Fig. 9, also the observation-based mean volume transport from the ARCGATE project (Tsubouchi et al., 2019; Tsubouchi et al., 2012, 2018) is given. To compare the ARCGATE value to ORAS5 and GREP, mean values and NRMSEs are calculated over the ARCGATE period (10/2004 - 05/2010, indicated by a *). With an annual mean volume transport of $0.151Sv$ the ARCGATE estimate is about 25% lower than the GREP estimate. The high NRMSE values emerge as the observation based ARCGATE flux does not show any peaks in June but rather stays low throughout the summer (not shown). This is probably a result from the mooring arrays in the gateways being too sparse and hence the velocity field not being measured accurately enough to dissolve the barotropic wave signal. Instead ARCGATE shows the export of freshwater that travels with the oceanic currents, dilutes on the way and remains around the continental shelfs for some time. Hence the oceanic reanalyses and the observation based ARCGATE estimate should only be compared in terms of annual means and not seasonalities.

4.3.1 Volumetric budget closure

To close the volumetric budget and get rid of the small residual we use a variational adjustment procedure (see Sect. 2.1.2). A priori estimates are calculated by taking the mean over all trustworthy estimates of the individual budget terms - given in Table

https://doi.org/10.5194/hess-2021-318
Preprint. Discussion started: 29 June 2021

Hydrology and Earth System Sciences
Discussions
Open Access
EGU

7. We perform the adjustment upon long term annual means to close the annual budget and upon the monthly climatologies of the individual terms to close the budget on a monthly scale. The uncertainties for the annual optimization are estimated as the standard deviations between the various estimates (see Table 7) of the mean annual budget terms. The uncertainties for the monthly optimization are estimated by taking the annual maximum of the monthly standard deviations, indicated by the dashed lines in Fig. 11. Oceanic lateral transport F features the largest uncertainties and hence also experiences the largest adjustments amongst all budget terms.

Figure 12 shows the adjusted long term annual volume budget over the oceanic and land domains. About $6584 \pm 84 km^3$

F	GREP
R	Obs$_{Ge}$, GloFAS$_{ERA5new}$,ERA5-Land
R$_{Greenland}$	Liquid and solid from Mankoff et al. (2020a, b)
Ocean$_{Atm,in}$	VIWVD from ERA5, ERA-Interim, JRA55, JRA55c
Ocean$_{stor}$	GRACE (CSR,GFZ,JPL)
Land$_{Atm,in}$	VIWVD from ERA5, ERA-Interim, JRA55, JRA55c
Land$_{stor}$	GRACE (CSR,GFZ,JPL)

Table 7. List of employed datasets in the variational adjustment procedure.

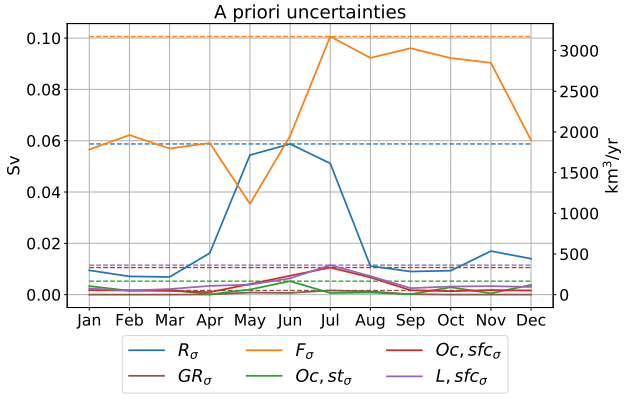

Figure 11. Mean annual cycles (1993-2018) of spread for runoff (R), Greenland runoff (GR), lateral ocean fluxes (F), oceanic storage (Oc,st) and atmospheric input over ocean (Oc,sfc) and land (L,sfc). Spread is calculated as standard deviate between various estimates (see table 7) of the individual terms and as RMS error estimate for GRACE.

leave the Arctic Ocean through the main gateways on an annual basis, whereof approximately $23 \pm 6 km^3$ are the result of a slight decline in the oceans volume storage. The remaining $6561 km^3$ enter the ocean via the surface, where roughly two thirds ($4379 \pm 25 km^3$) are supplied by runoff and about one third ($2182 \pm 80 km^3$) is delivered through the atmosphere. Oceanic transports out of the Arctic domain exceed the atmospheric moisture entering the Arctic ($6295 \pm 121 km^3$) by nearly 5%, indicating an annual loss of water volume of roughly $300 km^3$. The bulk part of this loss is generated through glacial melt and to a smaller part by surface drying of the Arctic land areas due to snow and permafrost degradation. Arctic land areas feature a

https://doi.org/10.5194/hess-2021-318
Preprint. Discussion started: 29 June 2021

Hydrology and Earth System Sciences
Discussions
Open Access
EGU

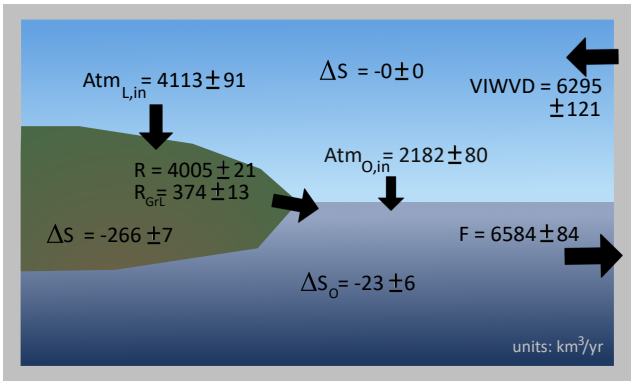

Figure 12. 1993-2018 adjusted long term means of the Arctics hydrological cycle. Units are km^3 per year; arrow areas are scaled by their magnitude.

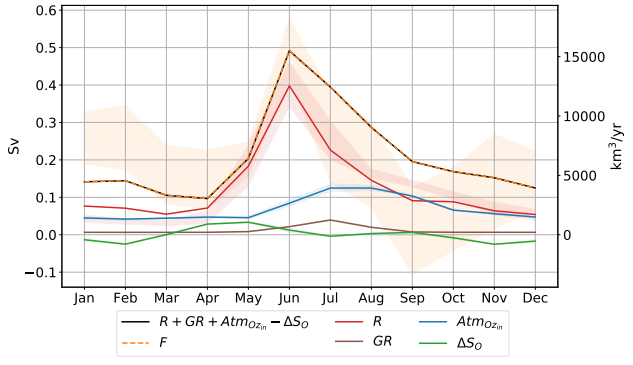

Figure 13. 1993-2018 adjusted mean annual cycle of the Arctic Oceans hydrological cycle. Shading represents the uncertainties of the a priori estimates.

decline of $266km^3$ per year, wherefrom approximately 50% come from Greenland, about 40% from Arctic glaciers (excluding Greenland) and the remaining 10% are the result of a decline in land water storage and snow cover. The reported slight decline in oceanic storage is probably caused due to variations generated by barotropic fluctuations forced by decadal wind variations/trends, while contributions from fresh water fluxes are assumed negligible (Volkov and Landerer, 2013; Fukumori et al., 2015). Volkov and Landerer (2013) find that an intensification of the westerly winds over the North Atlantic and over the Russian Arctic continental shelf lead to a decrease of ocean mass in the central Arctic. Further they show the correlation between Arctic Ocean mass fluctuations and northward wind anomalies over the Bering Seas and the northeastern North Atlantic. They reveal that cyclonic/anticyclonic anomalies of the large-scale ocean circulation lead to negative/positive Arctic mass anomalies.

Table 8 provides adjusted monthly and annual climatologies and Fig. 13 shows the adjusted seasonal cycles of the oceanic budget terms. A metric to identify whether the variational adjustment is successful is the comparison of the adjusted terms to

https://doi.org/10.5194/hess-2021-318
Preprint. Discussion started: 29 June 2021


Hydrology and Earth System Sciences
Discussions
Open Access
EGU

	R	GR	$Atm_{O,in}$	ΔS_O	F
Jan	2415	204	1420	-421	4460
Feb	2238	204	1320	-793	4554
Mar	1735	203	1396	9	3325
Apr	2250	207	1488	898	3047
May	5780	264	1438	1053	6428
Jun	12549	679	2660	393	15495
Jul	7137	1242	3935	-128	12441
Aug	4585	628	3933	101	9045
Sep	2868	234	3259	199	6163
Oct	2778	210	2073	-257	5317
Nov	2018	207	1773	-801	4800
Dec	1706	205	1491	-534	3937
Mean	4005	374	2182	-23	6584

Table 8. 1993-2018 adjusted mean annual cycle of the Arctic Oceans hydrological cycle; units are km^3 per year.

their a priori uncertainty (L'Ecuyer et al., 2015), hence Fig. 13 also shows the spreads of the a priori estimates (shaded areas). Due to the large differences between oceanic volume transports and freshwater input terms in late winter to early spring and in September, both F and runoff R feature adjustments beyond their a priori spreads, demonstrating that the a priori uncertainties are larger than indicated as systematic biases are not incorporated.

https://doi.org/10.5194/hess-2021-318
Preprint. Discussion started: 29 June 2021


Hydrology and Earth System Sciences
Discussions
Open Access
EGU

5 Conclusions

We analysed and compared various estimates of runoff into the Arctic Ocean on a seasonal and annual basis and find considerable differences in terms of seasonalities, mean values and trends. Further we used a non-steric formulation of the Arctics Ocean volume budget equation and compare freshwater input into the ocean to lateral volume transports over the Arctics boundaries. To close the budget and get best estimates of all budget terms we applied a variational adjustment procedure. The main outcomes of this study are the following:

- River discharge observations for the major Arctic catchments show distinct runoff peaks in June due to snow melt and river ice breakup and low runoff values in winter. Annual trends indicate slight discharge increases over the past decades - the largest increases evident at the Lena and Ob basins with a rise of about 4±2% per decade. The total Pan-Arctic area (excluding Greenland) exhibits an upward trend of 2±1% per decade. Holmes et al. (2018) show that the six largest Eurasian rivers (Ob, Yenisei,Lena, Kolyma, Pechora, Severnaya Dvina) exhibit an increase of 3.3±1.6% and the two largest North American rivers (Mackenzie and Yukon) an increase of 2.0±1.8% per decade.

- We estimate Pan-Arctic river discharge from gauge observations using monthly correction factors from GloFAS$_{ERA5new}$, as the popular method of hydrological analogy tends to underestimate the high flow summer peaks (see Fig. 4), and obtain a long term annual flux of 4031km^3 ± 203 (excluding Greenland).

- Runoff from ERA5 is substantially too low, with the largest errors occurring in the high flow summer months, and features strong declines of 10±1% per decade on a Pan-Arctic basis and even stronger declines at the major catchments. These strong and unrealistic declines can be traced back to two inhomogenities (1992 and 2004) present in ERA5s snow melt and are caused by the data assimilation system removing snow. While the discontinuity around 2004 was traced back to the introduction of the IMS snow cover information to the snow assimilation system, the 1992 inhomogeneity still needs further investigation.
  ERA5-Land does not feature these inhomogeneities and exhibits more moderate runoff declines of 5-6±2% for the Eurasian major watersheds and 2±1% for Mackenzie river and on the Pan-Arctic scale.

- Calculating runoff through the divergence of moisture flux is the only reanalyses based estimate that exhibits a slightly positive trend of 2 ± 1% per decade and thus features the best agreement with observations in terms of trends and the highest correlation coefficient. However VIWVD tends to underestimate runoff by roughly 5%.

- River discharge from GloFAS$_{ERA5}$ reflects the variation and the inhomogeneities from ERA5 and shows an additional negative shift due to two sink terms removing water in LISFLOOD that leads to a discharge underestimation of up to 50% towards the end of the time series. In contrast GloFAS$_{ERA5new}$ entails a vast improvement and reproduces the observed values best in terms of annual means and NRMSEs.

- Liquid and solid discharge from Greenland account for roughly 10% of total Pan-Arctic discharge and hence should not be neglected in assessments of the Arctic freshwater budget. Liquid discharge features a vast increase of 20±4% per

https://doi.org/10.5194/hess-2021-318
Preprint. Discussion started: 29 June 2021


Hydrology and Earth System Sciences
Discussions

decade and solid discharge an increase of $8\pm1\%$. Due to glacial melting also land storage changes are particularly strong over the Greenlandic ice sheet, accounting for roughly half of total Pan-Arctic land storage change.

- Comparing all trustworthy estimates of freshwater input into the Arctic Ocean to volume transports from ocean reanalysis yields only a small imbalance of 1% in terms of annual means.
- The variational adjustment procedure provides us with one best estimate of every budget term for every calendar month - listed in Tab. 8. About two thirds of the freshwater provided for oceanic volume transports come from runoff (4379±25 km^3 per year) and about one third is provided by the atmosphere. With oceanic and land storage declining - especially the land areas suffer a strong decline - there's a surplus of roughly $300km^3$ per year of more water leaving the Arctic area than entering.

Thus the variational adjustment brought reliable estimates of the volume budget terms on an annual scale, requiring only moderate adjustments of less than 1% for each individual term. With an annual value of 4379±25 km^3 (calculated over 1993-2018), our adjusted runoff estimate is slightly higher than estimates made by Shiklomanov and Lammers (2013) and Shiklomanov et al. (2021a) for the period 1936-2006. However considering the different calculation periods and assuming a decadal rise of roughly 2%, the estimates come quite close. On a seasonal scale however, the adjustment process was not a full success, as the budget residuals of some month are too large to be eliminated within the a priori spreads of the individual terms. This is very likely caused by systematic errors being present in the data-sets, or at least in their seasonal cycles, that are not taken into account in our a priori uncertainty estimates.

A possible reason for inconsistencies between runoff and ocean reanalyses is the usage of climatological river discharge data to specify land freshwater input in ocean reanalyses. Our analyses show that the seasonal cycle of the ORAS5 runoff climatology Bt06 fits quite well to our observation based estimates (see Fig. 5), however the lack of inter-annual variability in the freshwater input alters i.a. oceanic volume transports. In their BRONCO (Benefits of dynamically modelled river discharge input for ocean and coupled systems) project Zuo et al. (in preperation) work on implementing a time-varying land freshwater input, derived from discharge data from GloFAS version 2.1, into ORAS5. This should further reduce the inconsistencies between runoff and oceanic fluxes from ocean reanalyses.

In conclusion our results show that seasonal peaks of river discharge are underestimated in most reanalyses, mostly due to spurious signals in the data assimilation system. We find distinct improvements in the new GloFAS$_{ERA5new}$ product, especially when investigating seasonal cycles and long term means it features vast enhancements compared to its precursors. However for interannual variability and trend analysis we would recommend the use of the VIWVD estimate, as it reproduces trends from gauge observations quite accurately. In order to expand gauge observations onto the total Pan-Arctic area we would advise to use reliable river discharge estimates like GloFAS$_{ERA5new}$ to calculate discharge over the ungauged areas, as this results in more plausible seasonal cycles than the method of hydrological analogy. However in terms of trends and inter-annual

https://doi.org/10.5194/hess-2021-318
Preprint. Discussion started: 29 June 2021

variability the various observation based estimates (ae, Ge, Ee) show almost identical results, as the general trend is shaped by discharge from the major Arctic catchments.

Code and data availability. ERA5 and ERA5-Land data are available on the Copernicus Climate Change Service (C3S) Climate Data Store (Hersbach et al., 2019; Muñoz Sabater, 2019). GloFAS river discharge data are also available on the Copernicus Climate Change Service (C3S) Climate Data Store (Harrigan et al., 2019). GRACE monthly ocean bottom pressure anomalies and land water-equivalent-thickness anomalies are available through the Physical Oceanography Distributed Active Archive Center (Landerer, 2020b, a). River gauge observations are downloadable through the Arctic Great Rivers Observatory (Shiklomanov et al., 2021b) and the Regional Arctic Hydrographic Network data set (Lammers et al., 2001).

Appendix A: List of Acronyms

ARCGATE Mooring-derived data of oceanic fluxes through the Arctic gateways

BT06 runoff climatology used in ORAS5

BRONCO Benefits of dynamically modelled river discharge input for ocean and coupled atmosphere-land-ocean systems.

C3S Copernicus Climate Change Service

CAA Canadian Arctic Archipelago

CDS Climate Data Store

CGLORS ocean reanalyses from the Euro-Mediterranean Center on Climate Change

CMEMS Copernicus Marine Environment Monitoring Service

CEMS Copernicus Emergency Management Service

ECMWF European Centre for Medium-Range Weather Forecasts

ERA5 ECMWF's fifth atmospheric reanalysis

ERA5-Land offline simulation of ERA5

ERA-Interim ECMWF interim reanalysis

FOAM ocean reanalyses from the UK Met Office

GloFAS Global Flood Awareness System

GLORYS ocean reanalyses from Mercator Ocean

https://doi.org/10.5194/hess-2021-318
Preprint. Discussion started: 29 June 2021

GRACE Gravity Recovery and Climate Experiment

GREP Global ocean Reanalysis Ensemble Product

hbr0 experimental ORAS5 run using river discharge from GloFAS$_{ERA5}$

HTESSEL Hydrology Tiled ECMWF Scheme for Surface Exchanges over Land

JRA55 Japanese 55-year Reanalysis

JRC Joint Research Centre

LISFLOOD model for river basin scale water balance and flood simulation

NEMO Nucleus for European Modelling of the Ocean

NRMSE normalized root mean square error

Oras5 ECMWF's Ocean Reanalysis System 5

r Pearsons correlation coefficient

ET evapotranspiration

F oceanic lateral transport

$\mathbf{F}^{surf}$ freshwater surface fluxes (precipitation, evaporation, runoff)

g gravitational constant

P precipitation

p_s surface pressure

q specific humidity

R runoff or river discharge

rho_w density of freshwater

$\mathbf{S}_A$ atmospheric storage

$\mathbf{S}_L$ land storage

$\mathbf{S}_O$ ocean storage

SD snow depth

https://doi.org/10.5194/hess-2021-318
Preprint. Discussion started: 29 June 2021


Hydrology and Earth System Sciences
Discussions

SWVL Volumetric soil water per layer

v horizontal wind vector

VIWVD Vertical integral of divergence of moisture flux

Author contributions. S.W. performed the data analysis, including the production of the figures in the paper and prepared the manuscript. M.M., V.S., E.Z., H.Z. and L.H. contributed to the interpretation of results and the writing of the manuscript.

Competing interests. The authors declare that they have no conflict of interest.

Acknowledgements. The authors thank Takamasa Tsubouchi for the helpful discussions on ARCGATE data. S.W., V.S., and M.M. were supported by Austrian Science Fund project P33177. V.S. was additionally supported by Copernicus Marine environment Service contract 114- R&D-GLO-RAN-CMEMS Lot 8.

https://doi.org/10.5194/hess-2021-318
Preprint. Discussion started: 29 June 2021

References

Aagaard, K. and Carmack, E. C.: The role of sea ice and other fresh water in the Arctic circulation, Journal of Geophysical Research: Oceans, 94, 14 485–14 498, https://doi.org/10.1029/JC094iC10p14485, 1989.

Bacon, S., Aksenov, Y., Fawcett, S., and Madec, G.: Arctic mass, freshwater and heat fluxes: methods and modelled seasonal variability, Phil. Trans. R. Soc. A, 373, https://doi.org/10.1098/rsta.2014.0169, 2015.

Balsamo, G., Beljaars, A., Scipal, K., Viterbo, P., van den Hurk, B., Hirschi, M., and Betts, A. K.: A Revised Hydrology for the ECMWF Model: Verification from Field Site to Terrestrial Water Storage and Impact in the Integrated Forecast System, Journal of Hydrometeorology, 10, 623 – 643, https://doi.org/10.1175/2008JHM1068.1, 2009.

Blockley, E. W., Martin, M. J., McLaren, A. J., Ryan, A. G., Waters, J., Lea, D. J., Mirouze, I., Peterson, K. A., Sellar, A., and Storkey, D.: Recent development of the Met Office operational ocean forecasting system: an overview and assessment of the new Global FOAM forecasts, Geoscientific Model Development, 7, 2613–2638, https://doi.org/10.5194/gmd-7-2613-2014, 2014.

Bourdalle-Badie, R. and Treguier, A.-M.: A climatology of runoff for the global ocean-ice model ORCA025, 2006.

Burek, P., Van der Knijff, J., and De Roo, A.: LISFLOOD - Distributed Water Balance and Flood Simulation Model - Revised User Manual 2013, https://doi.org/10.2788/24982, 2013.

Church, J., Clark, P., Cazenave, A., Gregory, J., Jevrejeva, S., Levermann, A., Merrifield, M., Milne, G., Nerem, R., Nunn, P., Payne, A., Pfeffer, W., Stammer, D., and Unnikrishnan, A.: Sea Level Change. In: Climate Change 2013: The Physical Science Basis. Contribution of Working Group I to the Fifth Assessment Report of the Intergovernmental Panel on Climate Change [Stocker, T.F., D. Qin, G.-K. Plattner, M. Tignor, S.K. Allen, J. Boschung, A. Nauels, Y. Xia, V. Bex and P.M. Midgley (eds.)], Cambridge University Press, 2013.

Collins, M., Knutti, R., Arblaser, J., Dufresne, J.-L., Fichefet, T., Friedlingstein, P., Gao, X., Gutowski, W., Johns, T., Krinner, G., Shongwe, M., Teballdi, C., Weaver, A., and Wehner, M.: Long-term Climate Change: Projections, Commitments and Irreversibility, pp. 1029–1136, 2014.

Cucchi, M., Weedon, G. P., Amici, A., Bellouin, N., Lange, S., Müller Schmied, H., Hersbach, H., and Buontempo, C.: WFDE5: bias-adjusted ERA5 reanalysis data for impact studies, Earth System Science Data, 12, 2097–2120, https://doi.org/10.5194/essd-12-2097-2020, 2020.

Curry, B., Lee, C. M., and Petrie, B.: Volume, Freshwater, and Heat Fluxes through Davis Strait, 2004–05, Journal of Physical Oceanography, 41, 429 – 436, https://doi.org/10.1175/2010JPO4536.1, 2011.

Dee, D. P., Uppala, S. M., Simmons, A. J., Berrisford, P., Poli, P., Kobayashi, S., Andrae, U., Balmaseda, M. A., Balsamo, G., Bauer, P., Bechtold, P., Beljaars, A. C. M., van de Berg, L., Bidlot, J., Bormann, N., Delsol, C., Dragani, R., Fuentes, M., Geer, A. J., Haimberger, L., Healy, S. B., Hersbach, H., Hólm, E. V., Isaksen, L., Kållberg, P., Köhler, M., Matricardi, M., McNally, A. P., Monge-Sanz, B. M., Morcrette, J.-J., Park, B.-K., Peubey, C., de Rosnay, P., Tavolato, C., Thépaut, J.-N., and Vitart, F.: The ERA-Interim reanalysis: configuration and performance of the data assimilation system, Quarterly Journal of the Royal Meteorological Society, 137, 553–597, https://doi.org/10.1002/qj.828, 2011.

Desportes, C., Garric, G., Régnier, C., Drévillon, M., Parent, L., Drillet, Y., Masina, S., Storto, A., Mirouze, I., Cipollone, A., Zuo, H., Balmaseda, M., Peterson, D., Wood, R., Jackson, L., Mulet, S., and Greiner, E.: CMEMS-GLO-QUID-001-026, E.U. Copernicus Marine Service Information, 2017.

Dickson, R., Rudels, B., Dye, S., Karcher, M., Meincke, J., and Yashayaev, I.: Current estimates of freshwater flux through Arctic and subarctic seas, Progress in Oceanography, 73, 210–230, https://doi.org/10.1016/j.pocean.2006.12.003, 2007.

https://doi.org/10.5194/hess-2021-318
Preprint. Discussion started: 29 June 2021

Fukumori, I., Wang, O., Llovel, W., Fenty, I., and Forget, G.: A near-uniform fluctuation of ocean bottom pressure and sea level across the deep ocean basins of the Arctic Ocean and the Nordic Seas, Progress in Oceanography, 134, 152–172, https://doi.org/10.1016/j.pocean.2015.01.013, 2015.

Garric, G., Parent, L., Greiner, E., Drévillon, M., Hamon, M., Lellouche, J.-M., Régnier, C., Desportes, C., Le Galloudec, O., Bricaud, C., Drillet, Y., Hernandez, F., and Le Traon, P.-Y.: Performance and quality assessment of the global ocean eddy-permitting physical reanalysis GLORYS2V4., in: EGU General Assembly Conference Abstracts, EGU General Assembly Conference Abstracts, p. 18776, 2017.

Haine, T. W., Curry, B., Gerdes, R., Hansen, E., Karcher, M., Lee, C., Rudels, B., Spreen, G., de Steur, L., Stewart, K. D., and Woodgate, R.: Arctic freshwater export: Status, mechanisms, and prospects, Global and Planetary Change, 125, 13–35, https://doi.org/10.1016/j.gloplacha.2014.11.013, 2015.

Haine, T. W. N.: Arctic Ocean Freshening Linked to Anthropogenic Climate Change: All Hands on Deck, Geophysical Research Letters, 47, https://doi.org/10.1029/2020GL090678, 2020.

Harrigan, S., Zsoter, E., Barnard, C., F., W., Salamon, P., and Prudhomme, C.: River discharge and related historical data from the Global Flood Awareness System, v2.1, https://doi.org/10.24381/cds.a4fdd6b9, 2019.

Harrigan, S., Zsoter, E., Alfieri, L., Prudhomme, C., Salamon, P., Wetterhall, F., Barnard, C., Cloke, H., and Pappenberger, F.: GloFAS-ERA5 operational global river discharge reanalysis 1979–present, Earth System Science Data, 12, 2043–2060, https://doi.org/10.5194/essd-12-2043-2020, 2020.

Hersbach, H., Bell, B., Berrisford, P., Biavati, G., Horányi, A., Muñoz Sabater, J., Nicolas, J., Peubey, C., Radu, R., Rozum, I., Schepers, D., Simmons, A., Soci, C., Dee, D., and Thépaut, J.-N.: ERA5 monthly averaged data on single levels from 1979 to present, https://doi.org/10.24381/cds.f17050d7, 2019.

Hersbach, H., Bell, B., Berrisford, P., Hirahara, S., Horányi, A., Muñoz-Sabater, J., Nicolas, J., Peubey, C., Radu, R., Schepers, D., Simmons, A., Soci, C., Abdalla, S., Abellan, X., Balsamo, G., Bechtold, P., Biavati, G., Bidlot, J., Bonavita, M., De Chiara, G., Dahlgren, P., Dee, D., Diamantakis, M., Dragani, R., Flemming, J., Forbes, R., Fuentes, M., Geer, A., Haimberger, L., Healy, S., Hogan, R. J., Hólm, E., Janisková, M., Keeley, S., Laloyaux, P., Lopez, P., Lupu, C., Radnoti, G., de Rosnay, P., Rozum, I., Vamborg, F., Villaume, S., and Thépaut, J.-N.: The ERA5 global reanalysis, Quarterly Journal of the Royal Meteorological Society, 146, 1999–2049, https://doi.org/10.1002/qj.3803, 2020.

Holmes, R., Shiklomanov, A., Suslova, A., Tretiakov, M., McClelland, J., Spencer, R., and Tank, S.: River Discharge, Arctic Report Card: Update for 2018, https://arctic.noaa.gov/Report-Card/Report-Card-2018/ArtMID/7878/ArticleID/786/River-Discharge, 2018.

Knijff, J. M. V. D., Younis, J., and Roo, A. P. J. D.: LISFLOOD: a GIS-based distributed model for river basin scale water balance and flood simulation, International Journal of Geographical Information Science, 24, 189–212, https://doi.org/10.1080/13658810802549154, 2010.

Kobayashi, C., Endo, H., Ota, Y., Kobayashi, S., Onoda, H., Harada, Y., Onogi, K., and Kamahori, H.: Preliminary Results of the JRA-55C, an Atmospheric Reanalysis Assimilating Conventional Observations Only, SOLA, 10, 78–82, https://doi.org/10.2151/sola.2014-016, 2014.

Kobayashi, S., Ota, Y., Harada, Y., Ebita, A., Moriya, M., Onoda, H., Onogi, K., Kamahori, H., Kobayashi, C., Endo, H., Miyaoka, K., and Takahashi, K.: The JRA-55 Reanalysis: General Specifications and Basic Characteristics, Journal of the Meteorological Society of Japan. Ser. II, 93, 5–48, https://doi.org/10.2151/jmsj.2015-001, 2015.

Lammers, R. B., Shiklomanov, A. I., Vörösmarty, C. J., Fekete, B. M., and Peterson, B. J.: Assessment of contemporary Arctic river runoff based on observational discharge records, Journal of Geophysical Research: Atmospheres, 106, 3321–3334, https://doi.org/10.1029/2000JD900444, 2001.

Landerer, F.: CSR TELLUS GRACE Level-3 Monthly Ocean Bottom Pressure Anomaly RL06 v03, https://doi.org/10.5067/TEOCN-3AC63, 2020a.

Landerer, F.: CSR TELLUS GRACE Level-3 Monthly Land Water-Equivalent-Thickness Surface Mass Anomaly RL06 v03, https://doi.org/10.5067/TELND-3AC63, 2020b.

Lin, X., Massonnet, F., Yang, C., Artale, V., de Toma, V., and Rana, A.: Arctic freshwater cycle and the interaction with the North Atlantic, https://doi.org/10.5194/egusphere-egu21-436, eGU General Assembly 2021, online, 19–30 Apr 2021, EGU21-436, 2021.

L'Ecuyer, T. S., Beaudoing, H. K., Rodell, M., Olson, W., Lin, B., Kato, S., Clayson, C. A., Wood, E., Sheffield, J., Adler, R., Huffman, G., Bosilovich, M., Gu, G., Robertson, F., Houser, P. R., Chambers, D., Famiglietti, J. S., Fetzer, E., Liu, W. T., Gao, X., Schlosser, C. A., Clark, E., Lettenmaier, D. P., and Hilburn, K.: The Observed State of the Energy Budget in the Early Twenty-First Century, Journal of Climate, 28, 8319 – 8346, https://doi.org/10.1175/JCLI-D-14-00556.1, 2015.

Madec, G. and Team, N. S.: NEMO ocean engine, https://doi.org/10.5281/zenodo.1464816, 2019.

Mankoff, K. D., Noël, B., Fettweis, X., Ahlstrøm, A. P., Colgan, W., Kondo, K., Langley, K., Sugiyama, S., van As, D., and Fausto, R. S.: Greenland liquid water discharge from 1958 through 2019, Earth System Science Data, 12, 2811–2841, https://doi.org/10.5194/essd-12-2811-2020, 2020a.

Mankoff, K. D., Solgaard, A., Colgan, W., Ahlstrøm, A. P., Khan, S. A., and Fausto, R. S.: Greenland Ice Sheet solid ice discharge from 1986 through March 2020, Earth System Science Data, 12, 1367 – 1383, https://doi.org/10.5194/essd-12-1367-2020, 2020b.

Mayer, M., Alonso Balmaseda, M., and Haimberger, L.: Unprecedented 2015/2016 Indo-Pacific Heat Transfer Speeds Up Tropical Pacific Heat Recharge, Geophysical Research Letters, 45, 3274–3284, https://doi.org/10.1002/2018GL077106, 2018.

Mayer, M., Tietsche, S., Haimberger, L., Tsubouchi, T., Mayer, J., and Zuo, H.: An Improved Estimate of the Coupled Arctic Energy Budget, Journal of Climate, 32, 7915 – 7934, https://doi.org/10.1175/JCLI-D-19-0233.1, 2019.

Morison, J., Kwok, R., Peralta Ferriz, C., Alkire, M., Rigor, I., Andersen, R., and Steele, M.: Changing Arctic Ocean freshwater pathways, Nature, 481, 66–70, https://doi.org/10.1038/nature10705, 2012.

Muñoz Sabater, J., Dutra, E., Agustí-Panareda, A., Albergel, C., Arduini, G., Balsamo, G., Boussetta, S., Choulga, M., Harrigan, S., Hersbach, H., Martens, B., Miralles, D. G., Piles, M., Rodríguez-Fernández, N. J., Zsoter, E., Buontempo, C., and Thépaut, J.-N.: ERA5-Land: A state-of-the-art global reanalysis dataset for land applications, Earth System Science Data Discussions, 2021, 1–50, https://doi.org/10.5194/essd-2021-82, 2021.

Müller Schmied, H., Adam, L., Eisner, S., Fink, G., Flörke, M., Kim, H., Oki, T., Portmann, F. T., Reinecke, R., Riedel, C., Song, Q., Zhang, J., and Döll, P.: Variations of global and continental water balance components as impacted by climate forcing uncertainty and human water use, Hydrology and Earth System Sciences, 20, 2877–2898, https://doi.org/10.5194/hess-20-2877-2016, 2016.

Muntjewerf, L., Petrini, M., Vizcaino, M., Ernani da Silva, C., Sellevold, R., Scherrenberg, M. D. W., Thayer-Calder, K., Bradley, S. L., Lenaerts, J. T. M., Lipscomb, W. H., and Lofverstrom, M.: Greenland Ice Sheet Contribution to 21st Century Sea Level Rise as Simulated by the Coupled CESM2.1-CISM2.1, Geophysical Research Letters, 47, https://doi.org/10.1029/2019GL086836, 2020.

Muñoz Sabater, J.: ERA5-Land monthly averaged data from 1981 to present, https://doi.org/10.24381/cds.68d2bb3, 2019.

Prowse, T. D. and Flegg, P. O.: The magnitude of river flow to the Arctic Ocean: dependence on contributing area, Hydrological Processes, 14, 3185–3188, https://doi.org/10.1002/1099-1085(200011/12)14:16/17<3185::AID-HYP170>3.0.CO;2-S, 2000.

Rawlins, M. A., Steele, M., Holland, M. M., Adam, J. C., Cherry, J. E., Francis, J. A., Groisman, P. Y., Hinzman, L. D., Huntington, T. G., Kane, D. L., Kimball, J. S., Kwok, R., Lammers, R. B., Lee, C. M., Lettenmaier, D. P., McDonald, K. C., Podest, E., Pundsack, J. W., Rudels, B., Serreze, M. C., Shiklomanov, A., Øystein Skagseth, Troy, T. J., Vörösmarty, C. J., Wensnahan, M., Wood, E. F., Woodgate, R.,

Yang, D., Zhang, K., and Zhang, T.: Analysis of the Arctic System for Freshwater Cycle Intensification: Observations and Expectations, Journal of Climate, 23, 5715 – 5737, https://doi.org/10.1175/2010JCLI3421.1, 2010.

Rodell, M., Beaudoing, H. K., L'Ecuyer, T. S., Olson, W. S., Famiglietti, J. S., Houser, P. R., Adler, R., Bosilovich, M. G., Clayson, C. A., Chambers, D., Clark, E., Fetzer, E. J., Gao, X., Gu, G., Hilburn, K., Huffman, G. J., Lettenmaier, D. P., Liu, W. T., Robertson, F. R., Schlosser, C. A., Sheffield, J., and Wood, E. F.: The Observed State of the Water Cycle in the Early Twenty-First Century, Journal of Climate, 28, 8289 – 8318, https://doi.org/10.1175/JCLI-D-14-00555.1, 2015.

Schauer, U. and Losch, M.: "Freshwater" in the Ocean is Not a Useful Parameter in Climate Research, Journal of Physical Oceanography, 49, 2309 – 2321, https://doi.org/10.1175/JPO-D-19-0102.1, 2019.

Serreze, M. C., Barrett, A. P., Slater, A. G., Woodgate, R. A., Aagaard, K., Lammers, R. B., Steele, M., Moritz, R., Meredith, M., and Lee, C. M.: The large-scale freshwater cycle of the Arctic, Journal of Geophysical Research: Oceans, 111, https://doi.org/10.1029/2005JC003424, 2006.

Shiklomanov, A. and Lammers, R.: 5.11 - Changing Discharge Patterns of High-Latitude Rivers, in: Climate Vulnerability, edited by Pielke, R. A., pp. 161–175, Academic Press, Oxford, https://doi.org/10.1016/B978-0-12-384703-4.00526-8, 2013.

Shiklomanov, A., Déry, S., Tretiakov, M., Yang, D., Magritsky, D., Georgiadi, A., and Tang, W.: River Freshwater Flux to the Arctic Ocean, pp. 703–738, https://doi.org/10.1007/978-3-030-50930-9_24, 2021a.

Shiklomanov, A., Holmes, R., McClelland, J., Tank, S., and R.G.M., S.: Arctic Great Rivers Observatory. Discharge Dataset, Version YYYYMMDD, https://www.arcticgreatrivers.org/data, 2021b.

Shiklomanov, A. I. and Vuglinsky, V. S.: Hydrological networks, https://www.arcticobserving.org/images/pdf/Workshops/4th_stpetersburg/slideshow/shiklomanov_ppt.pdf, 2008.

Shiklomanov, A. I., Lammers, R. B., and Vörösmarty, C. J.: Widespread decline in hydrological monitoring threatens Pan-Arctic Research, Eos, Transactions American Geophysical Union, 83, 13–17, https://doi.org/10.1029/2002EO000007, 2002.

Shiklomanov, I. and Shiklomanov, A.: Climatic Change and the Dynamics of River Runoff into the Arctic Ocean, Water Resources, 30, 593–601, https://doi.org/10.1023/B:WARE.0000007584.73692.ca, 2003.

Stahl, K., Tallaksen, L. M., Hannaford, J., and van Lanen, H. A. J.: Filling the white space on maps of European runoff trends: estimates from a multi-model ensemble, Hydrology and Earth System Sciences, 16, 2035–2047, https://doi.org/10.5194/hess-16-2035-2012, 2012.

Storto, A. and Masina, S.: C-GLORSv5: an improved multipurpose global ocean eddy-permitting physical reanalysis, Earth System Science Data, 8, 679–696, https://doi.org/10.5194/essd-8-679-2016, 2016.

Storto, A., Masina, S., Simoncelli, S., Iovino, D., Cipollone, A., Drevillon, M., Drillet, Y., Schuckmann, K., Parent, L., Garric, G., Greiner, E., Desportes, C., Zuo, H., Balmaseda, M., and Peterson, K.: The added value of the multi-system spread information for ocean heat content and steric sea level investigations in the CMEMS GREP ensemble reanalysis product, Climate Dynamics, 53, https://doi.org/10.1007/s00382-018-4585-5, 2019.

Syed, T. H., Famiglietti, J. S., Zlotnicki, V., and Rodell, M.: Contemporary estimates of Pan-Arctic freshwater discharge from GRACE and reanalysis, Geophysical Research Letters, 34, https://doi.org/10.1029/2007GL031254, 2007.

Tsubouchi, T., Bacon, S., Naveira Garabato, A. C., Aksenov, Y., Laxon, S. W., Fahrbach, E., Beszczynska-Möller, A., Hansen, E., Lee, C. M., and Ingvaldsen, R. B.: The Arctic Ocean in summer: A quasi-synoptic inverse estimate of boundary fluxes and water mass transformation, Journal of Geophysical Research: Oceans, 117, https://doi.org/doi.org/10.1029/2011JC007174, 2012.

https://doi.org/10.5194/hess-2021-318
Preprint. Discussion started: 29 June 2021

Tsubouchi, T., Bacon, S., Aksenov, Y., Garabato, A. C. N., Beszczynska-Möller, A., Hansen, E., de Steur, L., Curry, B., and Lee, C. M.: The Arctic Ocean Seasonal Cycles of Heat and Freshwater Fluxes: Observation-Based Inverse Estimates, Journal of Physical Oceanography, 48, 2029 – 2055, https://doi.org/10.1175/JPO-D-17-0239.1, 2018.

Tsubouchi, T., von Appen, W.-J., Schauer, U., Kanzow, T., Lee, C., Curry, B., de Steur, L., Ingvaldsen, R., and Woodgate, R. A.: The Arctic Ocean volume, heat and fresh water transports time series from October 2004 to May 2010, https://doi.org/10.1594/PANGAEA.909966, 2019.

Vaughan, D., Comiso, J., Allison, I., Carrasco, J., Kaser, G., Kwok, R., Mote, P., Murray, T., Paul, F., Ren, J., Rignot, E., Solomina, O., Steffen, K., and Zhang, T.: Observations: Cryosphere. In: Climate Change 2013: The Physical Science Basis. Contribution of Working Group I to the Fifth Assessment Report of the Intergovernmental Panel on Climate Change [Stocker, T.F., D. Qin, G.-K. Plattner, M. Tignor, S.K. Allen, J. Boschung, A. Nauels, Y. Xia, V. Bex and P.M. Midgley (eds.)], Cambridge University Press, 2013.

Volkov, D. L. and Landerer, F. W.: Nonseasonal fluctuations of the Arctic Ocean mass observed by the GRACE satellites, Journal of Geophysical Research: Oceans, 118, 6451–6460, https://doi.org/10.1002/2013JC009341, 2013.

Wouters, B., Gardner, A., and Moholdt, G.: Global Glacier Mass Loss During the GRACE Satellite Mission (2002-2016), Frontiers in Earth Science, 7, https://doi.org/10.3389/feart.2019.00096, 2019.

Yang, D., Ye, B., and L. Kane, D.: Streamflow changes over Siberian Yenisei River Basin, Journal of Hydrology, 296, 59–80, https://doi.org/10.1016/j.jhydrol.2004.03.017, 2004a.

Yang, D., Ye, B., and Shiklomanov, A.: Discharge Characteristics and Changes over the Ob River Watershed in Siberia, Journal of Hydrometeorology, 5, 595 – 610, https://doi.org/10.1175/1525-7541(2004)005<0595:DCACOT>2.0.CO;2, 2004b.

Yang, D., Zhao, Y., Armstrong, R., Robinson, D., and Brodzik, M.-J.: Streamflow response to seasonal snow cover mass changes over large Siberian watersheds, Journal of Geophysical Research: Earth Surface, 112, https://doi.org/10.1029/2006JF000518, 2007.

Ye, B., Yang, D., and Kane, D. L.: Changes in Lena River streamflow hydrology: Human impacts versus natural variations, Water Resources Research, 39, https://doi.org/10.1029/2003WR001991, 2003.

Zsótér, E., Cloke, H. L., Prudhomme, C., Harrigan, S., de Rosnay, P., Munoz-Sabater, J., and Stephens, E.: Trends in the GloFAS-ERA5 river discharge reanalysis, https://doi.org/10.21957/p9jrh0xp, 2020.

Zuo, H., Alonso-Balmaseda, M., Mogensen, K., and Tietsche, S.: OCEAN5: The ECMWF Ocean Reanalysis System and its Real-Time analysis component, https://doi.org/10.21957/la2v0442, 2018.

Zuo, H., Balmaseda, M. A., Tietsche, S., Mogensen, K., and Mayer, M.: The ECMWF operational ensemble reanalysis–analysis system for ocean and sea ice: a description of the system and assessment, Ocean Science, 15, 779–808, https://doi.org/10.5194/os-15-779-2019, 2019.

Zuo, H., de Boisseson E., Zsoter, E., S., H., de Rosnay, P., and C., P.: Benefits of dynamically modelled river discharge input for ocean and coupled atmosphere-land-ocean systems, Journal of advances in modelling earth systems, in preperation.